Inorg. Chem. **1982**, *21*, 3666-3681

Contribution from Bell Laboratories,
Murray Hill, New Jersey 07974

Disulfur and Diselenium Complexes of Rhodium and Iridium

A. P. GINSBERG,* W. E. LINDSELL,[1] C. R. SPRINKLE, K. W. WEST, and R. L. COHEN

Received April 23, 1982

Coordinatively unsaturated low-valent rhodium and iridium complexes cleave S_8 and Se_8 rings and form complexes with the fragments. With square-planar $[M(L-L)_2]Cl$ ($M = Rh, Ir$; $L-L = (C_6H_5)_2PCH_2CH_2P(C_6H_5)_2$ (dppe), $(CH_3)_2PCH_2CH_2P(CH_3)_2$ (dmpe)) this reaction affords the monomeric electrolytes $[M(Y_2)(L-L)_2]Cl$ ($Y_2 = S_2, Se_2$). Oligomeric compounds are obtained from the reactions with $IrX(CO)(EPh_3)_2$ and $RhX(EPh_3)_3$ ($X = Cl, Br$; $E = P, As$); the products are $[\{Ir(Se_2)X(CO)(PPh_3)\}_3]$, $[\{Ir(Se_2)Cl(CO)(AsPh_3\}_3]$, $[\{IrS_6Cl(CO)(PPh_3)_2\}_n]$, $[\{RhS_3X(PPh_3)\}_4]$, $[\{RhSe_3Cl(PPh_3)\}_4]$, and $[\{RhY_2Cl(AsPh_3)\}_n]$ ($Y_2 = S_2, Se_2$). In the compounds $[M(Y_2)(L-L)_2]Cl$, disulfur and diselenium are side-on bonded to the metal at equatorial positions of a distorted octahedron. An X-ray structure determination of the diselenium complex $[Ir(Se_2)(dppe)_2]Cl\cdot H_2O\cdot 0.5C_6H_6$ shows the cation to be very similar to its dioxygen and disulfur analogues. The Se–Se distance is 2.312 (3) Å, about the same as the bond length in Se_8 and 0.16 Å longer than the Se–Se bond in the free Se_2 molecule. $[M(Y_2)(L-L)_2]^+$ complexes have ν(S–S) at 510–550 cm^{-1} and ν(Se–Se) at 300–310 cm^{-1}. The lowest energy feature of their electronic absorption spectra is a weak (ϵ 40–100 $M^{-1}\ cm^{-1}$) band assigned as an $a_2\pi_\perp^* \rightarrow b_1$ intraligand transition. $^{193}Ir(^1/_2+ \rightarrow {}^3/_2+)$ Mössbauer spectra of $[Ir(Y_2)(dppe)_2]Cl$ give isomer shifts that decrease along the series $Y_2 = O_2, S_2, Se_2$, in parallel with decreasing Y_2 electronegativity. The disulfur or diselenium group in $[M(Y_2)(L-L)_2]^+$ is readily reduced: mercury and tertiary phosphines strip sulfur or selenium from the complex with formation of HgS or HgSe and R_3PS or R_3PSe; the rate is very sensitive to the electronic environment of the disulfur or diselenium group and to the basicity of the phosphine. Low-valent group 8 metal complexes undergo oxidative addition across the S–S or Se–Se bond, allowing synthesis of the heterometallic $(\mu\text{-}S)_2$ dimers $[(dppe)_2Ir(\mu\text{-}S)_2PtL_2]X$ ($L = PPh_3$, $X = Cl$; $L = PEtPh_2$, $X = PF_6$) and $[(dmpe)_2Rh(\mu\text{-}S)_2Pt(PPh_3)_2]Cl$, as well as the asymmetric dimer $[(dppe)_2Ir(\mu\text{-}Se)_2IrCl(CO)(PEt_2Ph)_2]Cl$. Oxidative addition together with displacement of $[M(L-L)_2]^+$ by excess of the addend complex also occurs, giving homometallic $(\mu\text{-}S)_2$ or $(\mu\text{-}Se)_2$ dimers such as $[\{Ir(\mu\text{-}Se)Cl(CO)(PEt_2Ph)_2\}_2]$. Iodine adds across the S–S bond of $[Ir(S_2)(dppe)_2]Cl$ to form the novel cis-octahedral complex $[Ir(SI)_2(dppe)_2]Cl$.

Introduction[2]

Over the past decade there has been gradually increasing activity in the synthesis and structure determination of transition-metal disulfur and diselenium complexes.[3-29] It is now clear that disulfur can bond to metals in a variety of bridging geometries and also as a terminal group in the side-on manner[30]

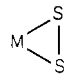

Examples of bridging[20] and terminal[5,21] side-on diselenium are also known. Unlike the case of the extensively investigated dioxygen complexes, there have been very few studies of the reactivity of metal-bonded disulfur and diselenium. We expect this to be an active area of research during the next several years, both because of the intrinsic interest of the chemistry of disulfur and diselenium ligands and because of the potential for reactions with these ligands to serve as a route for synthesizing new metal cluster complexes.

Most of the reactions of terminal side-on bonded disulfur and diselenium that have been reported involve oxidation of the S_2 or Se_2 group. For example, $[Ir(S_2)(dppe)_2]^+$ is oxidized by periodate to $[Ir(S_2O)(dppe)_2]^+$ and $[Ir(SO)_2(dppe)_2]^+$.[31,32] The same complex is methylated at the S_2 group by the strong electrophile CH_3SO_3F, forming $[Ir(S_2CH_3)(dppe)_2]^+$.[33] The latter reagent also methylates the S_2 group in $MoO(S_2)[S_2CN(CH_3)_2]_2$ to form $MoO(S_2CH_3)[S_2CN(CH_3)_2]_2$.[33] Methylation of the side-on S_2 or Se_2 in $Os(Y_2)(CO)_2(PPh_3)_2$ ($Y = S, Se$) takes place when the complexes are treated with $CH_3SO_3CF_3$.[14,21] In contrast to these reactions, the side-on dioxygen ligand is well-known to undergo reduction in its

---

(1) Present address: Department of Chemistry, Heriot-watt University, Edinburgh, U.K.

(2) The following abbreviations are used: Ph, C_6H_5; Et, C_2H_5; dppe, $(C_6H_5)_2P\ CH_2CH_2P(C_6H_5)_2$; dmpe, $(CH_3)_2PCH_2CH_2P(CH_3)_2$.

(3) P. M. Treichel and G. P. Werber, *J. Am. Chem. Soc.*, **90**, 1753 (1968).

(4) V. A. Uchtman and L. F. Dahl, *J. Am. Chem. Soc.*, **91**, 3756 (1969).

(5) A. P. Ginsberg and W. E. Lindsell, *Chem. Commun.*, 232 (1971).

(6) W. D. Bonds and J. A. Ibers, *J. Am. Chem. Soc.*, **94**, 3413 (1972).

(7) C. R. Brulet, S. S. Isied, and H. Taube, *J. Am. Chem. Soc.*, **95**, 4758 (1973).

(8) H. Siebert and S. Thym, *Z. Anorg. Allg. Chem.*, **399**, 107 (1973).

(9) A. Terzis and F. Rivest, *Inorg. Chem.*, **12**, 2132 (1973).

(10) J. Marcoll, A. Rabenau, D. Mootz, and H. Wunderlich, *Rev. Chim. Miner.*, **11**, 607 (1974).

(11) J. T. Mague and E. J. Davis, *Inorg. Chem.*, **16**, 131 (1977).

(12) R. C. Elder and M. Trkula, *Inorg. Chem.*, **16**, 1048 (1977).

(13) K. Mennemann and R. Mattes, *Angew. Chem., Int. Ed. Engl.*, **16**, 260 (1977).

(14) G. R. Clark, D. R. Russell, W. R. Roper, and A. Walker, *J. Organomet. Chem.*, **136**, C1 (1977).

(15) V. Kullmer, E. Rottinger, and H. Vahrenkamp, *J. Chem. Soc., Chem. Commun.*, 782 (1977).

(16) J. Dirand-Colin, M. Schappacher, L. Ricard, and R. Weiss, *J. Less-Common Met.*, **54**, 91 (1977).

(17) C. Giannotti, A. M. Ducourant, H. Chanaud, A. Chiaironi, and C. Riche, *J. Organomet. Chem.*, **140**, 289 (1977).

(18) H. Kopf, S. K. S. Hazari, and M. Leitner, *Z. Naturforsch., B*, **33B**, 1398 (1978).

(19) R. Rossetti, G. Gervasio, and P. L. Stanghellini, *Inorg. Chim. Acta*, **35**, 73 (1979).

(20) C. F. Campana, F. Y. Lo, and L. F. Dahl, *Inorg. Chem.*, **18**, 3060 (1979).

(21) D. H. Farrar, K. R. Grundy, N. C. Payne, W. R. Roper, and A. Walker, *J. Am. Chem. Soc.*, **101**, 6577 (1979).

(22) A. Muller, W. Eltzner, and N. Mohan, *Angew. Chem., Int. Ed. Engl.*, **18**, 168 (1979).

(23) W. Rittner, A. Muller, A. Neumann, W. Bather, and R. C. Sharma, *Angew. Chem., Int. Ed. Engl.*, **18**, 530 (1979).

(24) A. Muller, R. G. Bhattacharyya, and B. Pfefferkorn, *Chem. Ber.*, **112**, 778 (1979).

(25) A. Muller, W. O. Nolte, and B. Krebs, *Inorg. Chem.*, **19**, 2835 (1980).

(26) A. Muller and U. Reinsch, *Angew. Chem., Int. Ed. Engl.*, **19**, 72 (1980).

(27) C. Potvin, J. Bregeault, and J. Manoli, *J. Chem. Soc., Chem. Commun.*, 664 (1980).

(28) J. Ellermann, E. F. Hohenberger, W. Kehr, A. Purzer, and G. Thiele, *Z. Anorg. Allg. Chem.*, **464**, 45 (1980).

(29) H. Chanaud, A. M. Ducourant, and C. Giannotti, *J. Organomet. Chem.* **190**, 201 (1980).

(30) For a summary of types of metal–disulfur geometries see A. Muller and W. Jagermann, *Inorg. Chem.*, **18**, 2631 (1979).

(31) G. Schmid and G. Ritter, *Chem. Ber.*, **108**, 3008 (1975).

(32) G. Schmid and G. Ritter, *Angew. Chem., Int. Ed. Engl.*, **14**, 645 (1975).

(33) K. Leonard, K. Plute, R. C. Haltiwanger, and M. R. DuBois, *Inorg. Chem.*, **18**, 3246 (1979).

0020-1669/82/1321-3666$01.25/0 © 1982 American Chemical Society

reactions. The only reductions of side-on disulfur or diselenium that have been reported are the reactions of $MoO(S_2)(S_2CNR)$ ($R = CH_3$, C_2H_5, n-C_3H_7) with nucleophiles (e.g., PPh_3) in which the S–S bond is cleaved and sulfur atoms transfer to the nucleophile.[33] Electrochemical reduction of $[Ir(Y_2)(dppe)_2]^+$ ($Y_2 = O_2$, S_2, Se_2) takes place according to the scheme[34]

$$[Ir(Y_2)(dppe)_2]^+ + e^- \rightarrow [Ir(dppe)_2]^+ + Y_2^-$$

and involves addition of an electron to an $M-Y_2$ antibonding LUMO, which has its largest component on the Y_2 group.[35] Molecular orbital calculations have shown that the Y_2 group *in the complex* is best described as a molecule with excited configuration $...(p\sigma)^2(\pi)^3(\pi^*)^3$.[35]

In the present paper we report a study of the side-on bonded disulfur and diselenium compounds $[M(Y_2)(L-L)_2]Cl$ (M = Rh, Ir; Y = S, Se; L–L = dppe, dmpe).[5] An X-ray structure determination on $[Ir(Se_2)(dppe)_2]Cl$ shows it to have a structure very similar to its dioxygen[36] and disulfur[6] analogues. Analytical and spectroscopic measurements on the $[M(Y_2)(L-L)_2]Cl$ complexes show them all to have structures similar to those of $[Ir(S_2)dppe)_2]Cl$ and $[Ir(Se_2)(dppe)_2]Cl$. These compounds are especially appropriate for investigating the reactivity of side-on metal-bonded disulfur and diselenium since they allow the effects of changes in the electronic environment on reactivity to be examined and since they permit comparisons with the reactivity of dioxygen analogues.

The S_2 or Se_2 group in $[M(Y_2)(L-L)_2]Cl$ readily undergoes reactions in which it is reduced. Thus, mercury and tertiary phosphines strip sulfur or selenium from the complex with the formation of HgS or HgSe and R_3PS or R_3PSe. The rate of these reactions is very sensitive to the electronic environment of the disulfur or diselenium group and to the basicity of the phosphine. Corresponding reactions occur with dioxygen complexes. An especially interesting reduction of the disulfur or diselenium ligand is the oxidative addition of low-valent group 8 metal complexes across the S–S or Se–Se bond. This reaction enables the directed synthesis of heterometallic $(\mu\text{-}S)_2$ dimers. In this way we have obtained $[(dppe)_2Ir(\mu\text{-}S)_2PtL_2]X$ ($L = PPh_3$, X = Cl; $L = PEtPh_2$, $X = PF_6$) and $[(dmpe)_2Rh(\mu\text{-}S)_2Pt(PPh_3)_2]Cl$ as well as $[(dppe)_2Ir(\mu\text{-}Se)_2IrCl(CO)(PEt_2Ph)_2]Cl$. Oxidative addition together with displacement of $[M(L-L)_2]^+$ by excess of the addend complex also occurs, giving homometallic $(\mu\text{-}S)_2$ or $(\mu\text{-}Se)_2$ dimers such as $[\{Ir(\mu\text{-}Se)Cl(CO)(PEt_2Ph)_2\}_2]$. Analogous insertion reactions of low-valent metal species into the S–S or Se–Se bond of bridging disulfur or diselenium in the complexes $Fe_2(\mu\text{-}Y_2)(CO)_6$ (Y = S, Se) have recently been reported.[37,38] Corresponding reactions with dioxygen complexes are not known.

In addition to the work on $[M(Y_2)(L-L)_2]^+$ complexes outlined above, we also report the preparation of several new rhodium and iridium complexes containing bridging disulfur and diselenium from the reaction of $IrCl(CO)(EPh_3)_2$ (E = P, As) and $RhX(EPh_3)_3$ (X = Cl, Br; E = P; X = Cl; E = As) with S_8 or Se_8.

Experimental Section

Unless otherwise noted, all procedures were carried out by Schlenk techniques under a nitrogen or argon atmosphere or in a He-filled Vacuum Atmospheres drybox equipped with a recirculating system. Reagent grade solvents were distilled under nitrogen after drying as follows: benzene, toluene, hexane, and heptane with sodium wire, diethyl ether and tetrahydrofuran with lithium aluminum hydride, dichloromethane with phosphorus pentoxide, and acetonitrile with calcium hydride. Melting points were determined in evacuated tubes and are uncorrected. Analyses were performed by the Analytische Laboratorien, Engelskirchen, West Germany, Schwarzkopf Laboratory, Woodside, NY, and Galbraith Laboratories, Knoxville, TN.

Starting Materials. $[IrCl(CO)(PPh_3)_2]$ was purchased from Strem Chemical Co. and used as received. The following complexes were prepared by literature methods: $[RhX(PPh_3)_3]$ (X = Cl, Br),[39] $[Rh(dmpe)_2]Cl$,[40] $[Rh(dppe)_2]Cl$,[40] $[IrBr(CO)(PPh_3)_2]$,[41] $[IrCl(CO)(PEt_2Ph)_2]$,[42] $[IrCl(CO)(AsPh_3)_2]$,[42] $[Ir(dppe)_2]Cl$,[43] $[Pt(PPh_3)_3]$,[44] and $[RhCl(AsPh_3)_3]$.[45] $[Ir(dmpe)_2]Cl$ was obtained by refluxing $[\{IrCl(C_8H_{14})_2\}_2]$ with the stoichiometric amount of dmpe in benzene solution. $[Pt(PEtPh_2)_4]$ and $[Pt(PEtPh_2)_3]$ were prepared by the method described for the analogous PEt_3 complexes.[46] Orthorhombic sulfur was recrystallized from benzene before use. Monoclinic red selenium was obtained by Soxhlet extraction with CS_2 of either commercial red selenium or the product from the SO_2 reduction of selenous acid.

Physical Measurements. Molecular weights were determined at 38 °C with a Hewlett-Packard 302B vapor pressure osmometer calibrated with benzil and with triphenylphosphine. Measurements were made at three or four different concentrations in the range 0.005–0.05 mmol/g. The molecular weights reported are the values obtained by linear least-squares extrapolation to zero concentration. Conductivities were determined at 25.0 ± 0.1 °C on a Serfass conductivity bridge, Model RCM 15B1. Measurements were made in acetonitrile, nitromethane, or nitrobenzene at four or five concentrations in the range 10^{-2}–10^{-4} mequiv/mL. The conductivity cell consisted of two 1-cm^2 platinized platinum electrodes separated by ~1 cm; it was calibrated with 0.10 M KCl solution.

Infrared spectra were recorded on Perkin-Elmer 457 (4000–300 cm^{-1}) and Beckman IR11 (400–80 cm^{-1}) instruments. In the range 4000–300 cm^{-1} samples were measured in pressed CsI disks, and the spectra were calibrated by reference to the spectrum of a polystyrene film. In the range 400–80 cm^{-1} samples were measured in Nujol mulls between polyethylene plates, and the spectra were calibrated by reference to part of the rotational spectrum of water vapor. Raman spectra were recorded with an instrument based on a Spex 1301 0.5-m double monochromator with a Spex 1419A Raman illuminator (90° scattering geometry) and a Spex PC-1 photometric readout system (ACA C31034 photomultiplier cooled to −30 °C). Samples were mounted as neat powders and were rotated at ~4000 rpm while being excited with either the 6471-Å krypton ion line or the 5145-Å argon ion line of a Spectra-Physics Model 164 ion laser. Visible and ultraviolet absorption spectra were obtained with a Cary Model 14R spectrophotometer. ^1H NMR spectra were measured at ambient temperature on a Bruker WH-90 spectrometer. Mössbauer spectra were obtained as described elsewhere[47] with both source and absorber at 4.2 K; the source γ ray was quadrupole split by 0.48 mm/s. The 73-keV transition in $^{193}Ir(^1/_2+ \rightarrow {}^3/_2+)$ was used in these experiments.

$[Ir(S_2)(dppe)_2]Cl$ (1). A solution of orthorhombic sulfur (200 mg, 0.78 mmol of S_8) in benzene (35 mL) was added to a solution of $[Ir(dppe)_2]Cl$ (400 mg, 0.39 mmol) in methylene chloride (20 mL). Precipitation began after approximately 30 min. The reaction mixture was stirred at room temperature for 16 h when the precipitate was filtered off, washed with benzene, and dried at room temperature (390 mg, 92%). Recrystallization from methylene chloride by addition of benzene or ethyl ether, or from acetonitrile by addition of ethyl ether, followed by drying at 82 °C (10^{-3} mm) gave the salmon pink microcrystalline product. Two distinct crystalline forms, prismatic

---

(34) B. K. Teo, A. P. Ginsberg, and J. C. Calabrese, *J. Am. Chem. Soc.*, **98**, 3027 (1976).

(35) A. P. Ginsberg, J. H. Osborne, and C. R. Sprinkle, *Inorg. Chem.*, in press.

(36) M. J. Nolte, E. Singleton, and M. Laing, *J. Am. Chem. Soc.*, **97**, 6396 (1975).

(37) D. Seyferth, R. S. Henderson, and M. K. Gallagher, *J. Organomet. Chem.*, **193**, C75 (1980).

(38) D. A. Lesch and T. B. Rauchfuss, *J. Organomet. Chem.*, **199**, C6 (1980).

(39) J. A. Osborn and G. Wilkinson, *Inorg. Synth.*, **10**, 67 (1967).

(40) S. A. Butter and J. Chatt, *J. Chem. Soc. A*, 1411 (1970). The procedure given here for $[Rh(dmpe)_2]Cl$ was also used to make $[Rh(dppe)_2]Cl$.

(41) P. B. Chock and J. Halpern, *J. Am. Chem. Soc.*, **88**, 3511 (1966).

(42) J. Chatt, N. P. Johnson, and B. L. Shaw, *J. Chem. Soc. A*, 604 (1967).

(43) L. Vaska and D. L. Catone, *J. Am. Chem. Soc.*, **88**, 5324 (1966).

(44) R. Ugo, F. Cariati, and G. LaMonica, *Inorg. Synth.*, **11**, 105 (1968).

(45) J. T. Mague and G. Wilkinson, *J. Chem. Soc. A*, 1736 (1966).

(46) T. Yoshida, T. Matsuda, and S. Otsuka, *Inorg. Synth.*, **19**, 107 (1979).

(47) A. P. Ginsberg, R. L. Cohen, F. J. Disalvo, and K. W. West, *J. Chem. Phys.*, **60**, 2657 (1974).

and platelike, are observed. Crystallization from acetonitrile by slow evaporation gives the complex as orange prisms of the monosolvate, $[Ir(S_2)(dppe)_2]Cl{\cdot}CH_3CN$.

$[Ir(Se_2)(dppe)_2]Cl$ (2). Monoclinic red selenium (620 mg, 0.98 mmol of Se_8) was added to a solution of $[Ir(dppe)_2]Cl$ (1.01 g, 0.986 mmol) in methylene chloride (80 mL), and the mixture was stirred at room temperature for 8 days. Unreacted selenium was filtered off, and ethyl ether (ca. 50 mL) was added to the dark green filtrate; the precipitate which formed was collected by filtration, washed with ethyl ether, and dried at room temperature (990 mg, 85%). Recrystallization from methylene chloride–benzene followed by drying at 82 °C (10^{-3} mm) gave the green crystalline product.

$[Ir(S_2)(dmpe)_2]Cl$ (3). A solution of orthorhombic sulfur (300 mg, 1.17 mmol of S_8) in benzene (180 mL) was added to a suspension of $[Ir(dmpe)_2]Cl$ (1.00 g, 1.89 mmol) in tetrahydrofuran (250 mL), and the mixture was stirred at room temperature for 48 h. The precipitate that formed was collected, reprecipitated from acetonitrile with ethyl ether, washed with benzene, and dried at 80 °C (10^{-3} mm) to give the light orange-yellow product (774 mg, 69%).

$[Rh(S_2)(dppe)_2]Cl$ (4). A solution of orthorhombic sulfur (270 mg, 1.05 mmol) in benzene (80 mL) was mixed with a solution of $[Rh(dppe)_2]Cl$ (891 mg, 0.95 mmol) in methylene chloride (48 mL), and the mixture was allowed to stand for 18 days. After filtration through a fine frit, the solution was concentrated to 40 mL under reduced pressure and stored in a refrigerator overnight. Filtration afforded 470 mg (50%) of the medium purple product, which was recrystallized from acetonitrile and dried at 100 °C (10^{-3} mm).

$[Rh(S_2)(dmpe)_2]Cl$ (5). A solution of orthorhombic sulfur (120 mg, 0.47 mmol of S_8) in benzene (30 mL) was added to a suspension of $[Rh(dmpe)_2]Cl$ (450 mg, 1.03 mmol) in tetrahydrofuran (100 mL), and the mixture was stirred at room temperature for 16 h. The orange solid that formed was collected, washed with benzene, and dried at 82 °C (10^{-3} mm) to give the light yellow-brown hygroscopic product (490 mg, 95%).

$[Rh(S_2)(dmpe)_2]PF_6$ (6). Excess purified NH_4PF_6 was added to an aqueous solution of complex **5**. The precipitate that formed was collected, washed with water, and dried in air; the yield was essentially quantitative. Recrystallization from CH_3CN by addition of ethyl ether, followed by drying at 82 °C (10^{-3} mm), gave the orange-yellow product.

$[Rh(Se_2)(dmpe)_2]Cl$ (7). Monoclinic red selenium (570 mg, 0.90 mmol of Se_8) was added to a solution of $[Rh(dmpe)_2]Cl$ (760 mg, 1.73 mmol) in 1:1 tetrahydrofuran–benzene (100 mL), and the mixture was stirred at room temperature for 12 days. The suspended solid was filtered off and extracted with acetonitrile (6 × 10 mL). Ethyl ether (ca. 150 mL) was added to the dark brown extract to give a dark green precipitate. This crude product contained a brown impurity. After reprecipitation from acetonitrile by addition of ethyl ether, it was dissolved in a minimum amount of acetonitrile and transferred onto a 1.5 × 20 cm column of acid alumina (Woelm, Activity I). Elution with 1% methanol in acetonitrile (200 mL) followed by 2% methanol in acetonitrile (50 mL) removed all of the green color while leaving behind the brown impurity. The eluate was filtered and stripped dry; the residue was recrystallized from acetonitrile–ether to give the bright green crystalline product (452 mg, 44%), which was dried at 56 °C (10^{-3} mm).

$[\{Ir(Se_2)Cl(CO)(PPh_3)\}_3]$ (8). Monoclinic red selenium (250 mg, 0.40 mmol of Se_8) was stirred with $[IrCl(CO)(PPh_3)_2]$ (500 mg, 0.64 mmol) in benzene (75 mL) at 50–60 °C for 12 h, followed by stirring at room temperature for a further 24 h. The mixture was filtered, and the filtrate was concentrated under reduced pressure. Addition of ethyl ether precipitated the crude product in 80–90% yield. This was reprecipitated from benzene by addition of ether, washed with ether, and dried at 82 °C (10^{-3} mm) to give the orange-brown product (300 mg, 69%). Attempts to grow single crystals by slow evaporation of an acetonitrile solution and by vapor diffusion of ethyl ether into a benzene solution were unsuccessful.

$[\{Ir(Se_2)Br(CO)(PPh_3)\}_3]$ (9). This compound was prepared from $[IrBr(CO)(PPh_3)_2]$ (500 mg) and monoclinic red selenium (250 mg) by the procedure for complex **8**. The product (120 mg, 27%) was orange-brown.

$[\{Ir(Se_2)Cl(CO)(AsPh_3)\}_3]$ (10). Monoclinic red selenium (300 mg, 0.47 mmol of Se_8) and $[IrCl(CO)(AsPh_3)_2]$ (600 mg, 0.69 mmol) were stirred in benzene (100 mL) at room temperature for 12 h. The reaction mixture was then heated to 60 °C for 1.5 h, cooled, and filtered. The filtrate was worked up and the product purified as in the preparation of complex **8** to yield a light brown solid.

$[\{IrS_6Cl(CO)(PPh_3)_2\}_n]$ (11). Orthorhombic sulfur (600 mg, 2.34 mmol of S_8) in benzene (75 mL) and $[IrCl(CO)(PPh_3)_2]$ (600 mg, 0.77 mmol) in benzene (75 mL) were mixed at ambient temperature and left standing for 24 h. The yellow precipitate that formed was collected, washed with methylene chloride and then ether, and dried at 82 °C (10^{-3} mm); yield 190 mg (25%). The product was too insoluble for osmometric molecular weight determination. Other complexes containing Ir, S, PPh_3, and CO were formed in the reaction between S_8 and $[IrCl(CO)(PPh_3)_2]$ in benzene, but we were unable to characterize them.

$[\{RhS_3Cl(PPh_3)\}_4]$ (12). A solution of orthorhombic sulfur (120 mg, 0.47 mmol) in benzene (40 mL) was added to a solution of $RhCl(PPh_3)_3$ (500 mg, 0.54 mmol) in benzene (100 mL), and the mixture was left standing at room temperature for 5 h. The solution, which had turned dark red-brown, was filtered, and the filtrate was concentrated under reduced pressure. Addition of ethyl ether gave a precipitate which was collected (210 mg, 78%), dissolved in benzene, and reprecipitated by addition of ether. The brown product was washed with ether and dried at 82 °C (10^{-3} mm). Attempts to grow single crystals by slow evaporation of acetone and acetone–acetonitrile solutions and by vapor diffusion of ethyl ether into benzene, methylene chloride, and tetrahydrofuran solutions were all unsuccessful.

$[\{RhS_3Br(PPh_3)\}_4]$ (13). This compound was prepared in a manner similar to that for complex **12** from orthorhombic sulfur (200 mg, 0.78 mmol of S_8) and $RhBr(PPh_3)_3$ (500 mg, 0.52 mmol) in benzene solution. After 12 h at room temperature an ~75% yield of brown product was obtained.

$[\{RhSe_3Cl(PPh_3)\}_4]$ (14). Monoclinic red selenium (300 mg, 0.47 mmol of Se_8) was added to a solution of $[RhCl(PPh_3)_3]$ (500 mg, 0.54 mmol) in benzene (100 mL), and the mixture was heated to 60–70 °C for 2 h and then stirred at ambient temperature for 16 h. The deep red-brown solution was filtered and then concentrated under reduced pressure. Addition of ethyl ether gave a deep brown precipitate, which was collected, dissolved in benzene, and reprecipitated with ether. The brown-black product (150 mg, 44%) was washed with ether and dried at 82 °C (10^{-3} mm).

$[\{RhS_2Cl(AsPh_3)\}_n]$ (15). Orthorhombic sulfur (200 mg, 0.78 mmol of S_8) in benzene (50 mL) was added to a solution of $[RhCl(AsPh_3)_3]$ (400 mg, 0.38 mmol) in benzene (50 mL). The mixture was left at ambient temperature for 6 h and then worked up as in the preparation of compound **12** to give the brown product (90 mg, 47%).

$[\{RhSe_2Cl(AsPh_3)\}_n]$ (16). Monoclinic red selenium (300 mg, 0.47 mmol of Se_8) and $[RhCl(AsPh_3)_3]$ (600 mg, 0.57 mmol) were stirred in benzene (100 mL) at ambient temperature for 16 h. The reaction mixture was then heated at 60–70 °C for 2 h, cooled, and filtered. The filtrate was worked up as in the preparation of compound **12** to give 140 mg (41%) of brown-black product.

Reaction of $[\{RhS_3Cl(PPh_3)\}_4]$ with $AsPh_3$. $[\{RhS_3Cl(PPh_3)\}_4]$ (250 mg, 0.50 mmol of Rh) and $AsPh_3$ (4.0 g, 13 mmol) were refluxed in benzene solution for 6 days. The solution was concentrated under reduced pressure, and the product was precipitated by addition of ethyl ether. After reprecipitation from benzene–ether, it was dried at 82 °C (10^{-3} mm). An IR spectrum (CsI disk) showed weak bands (1095, 525 cm^{-1}) due to PPh_3 in the starting complex but was otherwise identical with the spectrum of $[\{RhS_2Cl(AsPh_3)\}_n]$. Analysis confirmed the characterization. Anal. Found: C, 42.59; H, 3.15; S, 12.82; As, 14.40; Cl, 6.79; P, 0.38.

Reaction of $[\{RhS_3Cl(PPh_3)\}_4]$ with PPh_3. $[\{RhS_3Cl(PPh_3)\}_4]$ (380 mg, 0.76 mmol of Rh) and PPh_3 (2.0 g, 7.6 mmol) were refluxed in benzene for 30 min. A brown solid precipitated on addition of ethyl ether to the cooled solution. This material was reprecipitated from benzene with ether, washed with ether, and dried at 82 °C (10^{-3} mm). Anal. Calcd for $[\{RhSCl(PPh_3)\}_n]$: C, 49.96; H, 3.49; S, 7.41; P, 7.16; Cl, 8.19. Found: C, 50.84; H, 3.80; S, 6.95; P, 7.04; Cl, 7.70.

Reaction of $[Ir(S_2)(dppe)_2]Cl$ with O_2. (a) A solution of $[Ir(S_2)(dppe)_2]Cl$ (100 mg) in dichloromethane (100 mL) was stirred under an oxygen atmosphere for 10 h. The dissolved material was recovered by precipitation with excess ether; IR spectroscopy showed it to be the unchanged starting complex.

(b) Solid $[Ir(S_2)(dppe)_2]Cl$ (50 mg) in a platinum tube was subjected to 650 atm pressure of oxygen for 52 h at 80 °C. The recovered material was unchanged in appearance, and its IR spectrum showed no evidence of oxidation. The experiment was repeated with 510 atm of oxygen for 6 days at 170 °C. The recovered material was dark brown-black and insoluble in organic solvents.

Reaction of [Ir(Se_2)(dppe)$_2$]Cl with O_2. [Ir(Se_2)(dppe)$_2$]Cl (46 mg) was dissolved in acetonitrile (20 mL). After its absorption spectrum (300–800 nm) was recorded, the solution was subjected to 4 atm of oxygen for 3 days at room temperature. The absorption spectrum of the recovered solution was unchanged.

Reaction of [Ir(Se_2)(dppe)$_2$]Cl with Hg. [Ir(Se_2)(dppe)$_2$]Cl (20 mg) was dissolved in acetonitrile (10 mL), and the solution was stirred with mercury (1 mL). After about 2 h the initially yellow-green solution had turned orange and a brown precipitate was present. After 12 h the absorption spectrum (300–800 nm) of the solution was that of [Ir(dppe)$_2$]Cl; no bands characteristic of the Se_2 adduct remained. The brown precipitate was recovered and identified as cubic HgSe from its X-ray powder pattern.

Relative Rates of Reaction of [M(Y_2)(L–L)$_2$]Cl Complexes with Hg. A 10–20-mL quantity of a (2–3) × 10^{-3} M solution of the complex in acetonitrile was vigorously stirred with 0.5 g of Hg in a closed tube (He atmosphere). At the end of 2 h it was evident that compounds **2**, **4**, and **6** had reacted extensively; these solutions were centrifuged and their optical spectra (300–800 nm) were measured. The other compounds showed no sign of reaction after 2 h; stirring was continued for 10 days before the spectrum of the solution was measured. From the decrease in intensity of bands characteristic of the S_2 or Se_2 complexes, or from the growth of bands due to [M(L–L)$_2$]$^+$, the percent conversion to [M(L–L)$_2$]$^+$ was estimated.

Reaction of [Ir(Se_2)(dppe)$_2$]Cl with PEtPh$_2$. [Ir(Se_2)(dppe)$_2$]Cl (31.3 mg, 0.0265 mmol) was added to a solution of PEtPh$_2$ (11.3 mg, 0.0527 mmol) in CH_3CN, and the mixture was diluted to 10.00 mL. The reaction was followed by periodically measuring the absorption spectrum (300–650 nm) until conversion to [Ir(dppe)$_2$]Cl was complete.

Reaction of [Ir(Se_2)(dppe)$_2$]Cl with PPh$_3$. (a) The same procedure was used as for PEtPh$_2$, and the reaction was followed for 4 days.

(b) [Ir(Se_2)(dppe)$_2$]Cl (317 mg, 0.268 mmol) and PPh$_3$ (141 mg, 0.538 mmol) were stirred in CH_3CN (25 mL) for 5 days. Acetonitrile was removed under reduced pressure, and the residue was extracted with toluene. The toluene extract was stripped and the residue taken up in benzene (10 mL). Addition of hexane (200 mL) to the filtered benzene solution gave a precipitate, which was collected after cooling at 0 °C for several hours. The pale yellow product (49 mg) was identified as Ph$_3$PSe by its IR spectrum (ν(PSe) = 559 cm^{-1}) and analysis.

Reaction of [Ir(S_2)(dppe)$_2$]Cl with PEtPh$_2$. The same procedure and concentrations were used as for the Se_2 complex, and the reaction was followed for 12 days.

[Ir(SI)$_2$(dppe)$_2$]Cl (17). Iodine (47 mg, 0.185 mmol of I_2) in dichloromethane (15 mL) was added to a solution of [Ir(S_2)(dppe)$_2$]Cl (200 mg, 0.184 mmol) in dichloromethane (10 mL). Benzene (75 mL) was added to the dark red-orange mixture after it had stood for 2.5 h at room temperature under the ambient atmosphere. Dark red crystals formed slowly and after 15 days were collected and washed with ethyl ether. Microscopic examination showed the crystals to be twinned or internally shattered; they were crushed to a dark brown powder and dried at 56 °C (10^{-3} mm); yield 190 mg (77%).

[(dppe)$_2$IrS$_2$Pt(PPh$_3$)$_2$]Cl (18). A solution of Pt(PPh$_3$)$_3$ (499 mg, 0.508 mmol) in tetrahydrofuran (10 mL) was added to a stirred solution of [Ir(S_2)(dppe)$_2$]Cl (552 mg, 0.507 mmol) in acetonitrile (75 mL). After addition of toluene (120 mL) the solution was concentrated to 30 mL under reduced pressure. The precipitate that formed was collected, washed with toluene, and dried at 100 °C (10^{-3} mm) to give the medium orange-yellow product (766 mg, 80%).

[(dppe)$_2$IrS$_2$Pt(PEtPh$_2$)$_2$]PF$_6$ (19). Pt(PEtPh$_2$)$_4$ (1.007 g, 0.957 mmol) was converted to Pt(PEtPh$_2$)$_3$ and dissolved in CH_3CN (10 mL). This solution was added to solid [Ir(S_2)(dppe)$_2$]Cl (1.042 g, 0.957 mmol) with additional CH_3CN (15 mL) to effect quantitative transfer. After being stirred for 0.5 h, the solution was filtered, and purified NH_4PF_6 (6 g) was added to the filtrate. The precipitate that formed was collected, washed with acetonitrile, and dried at 82 °C (10^{-3} mm) to give the light orange-yellow product (925 mg, 53%). NH_4Cl, which coprecipitated with the complex, was sublimed off during drying.

[(dmpe)$_2$RhS$_2$Pt(PPh$_3$)$_2$]Cl (20). A solution of [Pt(PPh$_3$)$_3$] (599 mg, 0.610 mmol) in tetrahydrofuran (10 mL) was added to a stirred solution of [Rh(S_2)(dmpe)$_2$]Cl (307 mg, 0.610 mmol) in acetonitrile (10 mL). After addition of toluene (120 mL) the solution was concentrated to 40 mL under reduced pressure. The precipitate that formed was collected, washed with toluene, and dried at 100 °C (10^{-3} mm) to give the strong yellow product (670 mg, 85%).

[{PtS(PPh$_3$)$_2$}$_n$] (21). [Pt(PPh$_3$)$_3$] (593 mg, 0.604 mmol) was added to a solution of [Ir(S_2)(dppe)$_2$]Cl (329 mg, 0.302 mmol) in acetonitrile (125 mL), and the mixture was stirred for 12 h. The precipitate was collected, washed with acetonitrile, and dried at 82 °C (10^{-3} mm) to give the orange-yellow product (448 mg, 99%). The comopund was too insoluble for molecular weight determination. The UV–visible spectrum of the filtrate confirmed that it contained all of the iridium as [Ir(dppe)$_2$]Cl.

[{PtS(PEtPh$_2$)$_2$}$_2$] (22). Pt(PEtPh$_2$)$_4$ (1.167 g, 1.109 mmol) was converted to Pt(PEtPh$_2$)$_3$, which was dissolved in acetonitrile (25 mL); the solution was added to [Ir(S_2)(dppe)$_2$]Cl (555 mg, 0.510 mmol), and the mixture was stirred until the iridium complex had dissolved. After standing for 2 days, the crystalline solid that had formed was collected, washed with acetonitrile, and dried at 100 °C (10^{-3} mm) to give the orange product (254 mg, 35%).

[{PtSe(PPh$_3$)$_2$}$_n$]·*n*C$_4$H$_8$O (23). Attempted Preparation of [(dppe)$_2$IrSe$_2$Pt(PPh$_3$)$_2$]PF$_6$. A solution of Pt(PPh$_3$)$_3$ (872 mg, 0.888 mmol) in 1:1 acetonitrile–tetrahydrofuran (50 mL) was added to a stirred solution of [Ir(Se_2)(dppe)$_2$]BPh$_4$[48] (1.302 g, 0.888 mmol) in the same solvent (100 mL). The green color of the Se_2 complex rapidly turned to a deep red, and precipitation took place. After 5 min the precipitate was collected, washed with 1:1 acetonitrile–tetrahydrofuran followed by neat acetonitrile, and dried at 55 °C (10^{-3} mm). The yellow-brown product (726 mg, 94%) was shown by X-ray fluorescence analysis to contain Pt but no Ir. It was too insoluble for molecular weight determination. Addition of 10 g of NH_4PF_6 to the filtrate failed to give a precipitate.

[{PtSe(PEtPh$_2$)$_2$}$_2$]·C$_7$H$_{16}$ (24). Solid [Pt(PEtPh$_2$)$_4$] (982 mg, 0.933 mmol) was added to a stirred solution of [Ir(Se_2)(dppe)$_2$]Cl (552 mg, 0.467 mmol) in acetonitrile (100 mL). The solution rapidly turned red and deposited a red crystalline precipitate. The latter was collected, washed with acetonitrile, and sucked dry (418 mg, 64%). Recrystallization from toluene (3 mL) by addition of heptane (80 mL) followed by drying at 25 °C (10^{-3} mm) gave the orange-red product. The red-brown solvent-free complex was obtained by drying at 100 °C (10^{-3} mm); mass spectrometric analysis of the liberated solvent showed it to be 80% heptane + 20% toluene.

[(dppe)$_2$IrSe$_2$Ir(CO)Cl(PEt$_2$Ph)$_2$]Cl (25). Solid [IrCl(CO)(PEt$_2$Ph)$_2$] (246 mg, 0.418 mmol) was added to a solution of [Ir(Se_2)(dppe)$_2$]Cl (496 mg, 0.420 mmol) in methylene chloride (30 mL), and the mixture was stirred at room temperature until an IR spectrum showed that the CO stretching band of the starting complex had disappeared (ca. 35 h). The clear solution was concentrated under reduced pressure to about 5 mL. Addition of excess ethyl ether gave an orange precipitate, which was collected and dried in a circulating He atmosphere (0.73 g, ca. 98%). Microscopic examination showed this material to contain about 10% [Ir(Se_2)(dppe)$_2$]Cl. Purification was effected by dissolving the crude material (0.36 g) in methylene chloride (5 mL) and filtering into 80 mL of toluene; the filtrate was concentrated (10^{-3} mm) to 20 mL, and the precipitate was collected, washed with toluene, and dried at 80 °C (10^{-3} mm) to give the orange-yellow product (0.18 g).

[{IrSeCl(CO)(PEt$_2$Ph)}$_2$] (26). Solid [IrCl(CO)(PEt$_2$Ph)$_2$] (735 mg, 1.25 mmol) was added to a stirred solution of [Ir(Se_2)(dppe)$_2$]Cl (739 mg, 0.625 mmol) in acetonitrile (100 mL; the Se_2 complex was not completely dissolved). The green color of the solution gradually changed to orange; after 24 h the precipitate that had formed was collected, washed with acetonitrile, and dried at 82 °C (10^{-3} mm) to give the orange product (572 mg, 69%).

X-ray Study of [Ir(Se_2)(dppe)$_2$]Cl·H$_2$O·0.5C$_6$H$_6$.[49] Single crystals suitable for X-ray diffraction were obtained by vapor diffusion of benzene into a solution of [Ir(Se_2)(dppe)$_2$]Cl (50 mg) in acetonitrile (8 mL) at 25 °C. *Undried* solvents were used and an inert atmosphere was *not* provided. The crystals, which lose solvent of crystallization and become opaque on standing in air, were mounted in glass capillaries in the mother liquor.

Preliminary precession photography showed the crystals to be monoclinic. Systematic absences (*hkl*, *h* + *k* odd; *h0l*, *l* odd) are consistent with the space groups C_s^4-*Cc* and C_{2h}^6-*C*2/*c*. Tests for

---

[48] Prepared by metathesis of [Ir(Se_2)(dppe)$_2$]Cl with NaBPh$_4$ in CH_3CN. Coprecipitated NaCl is removed by extraction with water.

[49] This structure determination was preformed by the crystallographic staff of the Molecular Structure Corp.: Dr. M. W. Extine, Ms. R. A. Meisner, and Dr. J. M. Troup.

Table I. Summary of Crystal Data and Intensity Collection for $[\mathrm{Ir(Se_2)(dppe)_2}]\mathrm{Cl \cdot H_2O \cdot 0.5C_6H_6}$

empirical formula	$C_{55}H_{53}ClIrSe_2OP_4$
fw	1239.50
cryst shape	prism
cryst dimens	0.20 × 0.21 × 0.22 mm
width at half-height from ω scans	0.30°
system	monoclinic
centering	*c* centered
space group	C_{2h}^6-$C2/c$
a	20.15 (1) Å
b	12.48 (1) Å
c	40.76 (2) Å
β	104.47 (8)°
V	9925 (10) Å^3
temp	23 ± 1°
d(calcd)	1.659 g/cm^3
d(obsd)	1.64 g/cm^3
Z	8
radiation	Mo Kα(λ = 0.710 73 Å)
μ	46.47 cm^{-1}
transmission coeff	0.370-0.394
crystal-to-detector dist	19 cm
counter aperture width	2.0 mm
incident-beam collimator diameter	1.5 mm
takeoff angle	3°
technique	ω scan
scan rate	4-24°/min
$R = t_{\mathrm{scan}}/t_{\mathrm{back}}$	2.0
range of data	$0° < 2\theta < 43°$
unique data, $F_o^2 > 3\sigma(F_o^2)$	3042
no. of atoms	65
final no. of variables	297
esd of observn of unit wt	1.233
R_1	0.055
R_2	0.069

piezoelectricity and second harmonic generation were negative, indicating the probable presence of a center of symmetry. The most likely space group is therefore C_{2h}^6-$C2/c$.

Table I summarizes the crystal data and intensity collection. Cell constants and their standard deviations were obtained by least-squares refinement of the setting angles of 15 computer-centered reflections. The calculated density for 8 formula units per unit cell is 1.659 g/cm^3, in reasonable agreement with the value 1.64 g/cm^3 determined by flotation in aqueous zinc chloride.

Intensity data were collected at 23 ± 1 °C on a Syntex P$\bar{1}$ diffractometer using Mo Kα radiation. The ω-scan technique was used with a variable scan rate of 4–24°/min. Stationary-crystal, stationary-counter background counts were taken at each end of a scan; the scan width was 1.5° centered around 2θ. Reflections were collected in the range $0° < 2\theta < 43°$, and a total of 5948 reflections, of which 5765 were unique, were obtained. Periodic checks of the intensities of these representative reflections showed no significant change with time. The formulas used to calculate the intensities and their standard deviations were

$$I = S(C - RB) \qquad \sigma(I) = [S^2(C + R^2B) + (pI)^2]^{1/2}$$

where S is the scan rate, C is the total integrated peak count, R is the ratio of scan time to background counting time, B is the total background count, and p is an empirical parameter that reduces the weight given to strong reflections ($p = 0.07$ was used). Corrections were applied to the data for Lorentz and polarization effects; a spherical absorption correction was also made.

Standard Patterson and Fourier techniques were used to solve the structure. Refinement was by the full-matrix least-squares method in space group $C2/c$. The function minimized in the refinement was $\sum w_i(|F_o| - |F_c|)^2$, where $|F_o|$ and $|F_c|$ are the observed and calculated structure amplitudes and w is the weighting function defined as $4F_o^2/\sigma^2(F_o^2)$. Values for the atomic scattering factors[50] and the anomalous terms[51] were from the usual sources. Only the 3042 unique reflections having $F_o^2 > 3\sigma(F_o^2)$ were used in the refinement. The Ir, Se, P, and Cl atoms were allowed to vibrate anisotropically, but the C atoms and the O atom of the water of solvation were assigned isotropic thermal parameters. Hydrogen atoms were not included in the refinement. Peaks suggesting the presence of benzene and water of crystallization appeared in difference Fourier maps at an intermediate stage in the refinement. These were included and refined well. The identity of the benzene molecule is confirmed by its final geometry and temperature factors. The water molecule appeared as a single peak, the assignment of which as H_2O is the only plausible possibility given the conditions under which the crystals were grown.

The final values for the least-squares residuals

$$R_1 = \sum||F_o| - |F_c||/\sum|F_o|$$

$$R_2 = [\sum w_i(|F_o| - |F_c|)^2/\sum w_i F_o^2]^{1/2}$$

are given in Table I. A final difference Fourier map had its largest peaks in positions expected for phenyl ring hydrogen atoms. An analysis of $\sum w_i(|F_o| - |F_c|)^2$ as a function of $|F_o|$, setting angles, and Miller indices showed no significant trends. A list of the observed and calculated structure factors is available.[52]

Results and Discussion

Synthesis and Reactions. *cyclo*-Octasulfur and *cyclo*-octaselenium react with rhodium and iridium bis(diphosphine) complexes as indicated in reactions 1–6 to form compounds

$$[\mathrm{Ir(dppe)_2}]\mathrm{Cl} + \mathrm{S_8} \xrightarrow[\mathrm{C_6H_6-CH_2Cl_2}]{16\ \mathrm{h}} \mathbf{1} \qquad (1)$$

$$[\mathrm{Ir(dppe)_2}]\mathrm{Cl} + \mathrm{Se_8} \xrightarrow[\mathrm{CH_2Cl_2}]{8\ \mathrm{days}} \mathbf{2} \qquad (2)$$

$$[\mathrm{Ir(dmpe)_2}]\mathrm{Cl} + \mathrm{S_8} \xrightarrow[\mathrm{C_6H_6-THF}]{48\ \mathrm{h}} \mathbf{3} \qquad (3)$$

$$[\mathrm{Rh(dppe)_2}]\mathrm{Cl} + \mathrm{S_8} \xrightarrow[\mathrm{C_6H_6-CH_2Cl_2}]{18\ \mathrm{days}} \mathbf{4} \qquad (4)$$

$$[\mathrm{Rh(dmpe)_2}]\mathrm{Cl} + \mathrm{S_8} \xrightarrow[\mathrm{C_6H_6-THF}]{16\ \mathrm{h}} \mathbf{5} \xrightarrow[\mathrm{PF_6^-}]{\mathrm{H_2O}} \mathbf{6} \qquad (5)$$

$$[\mathrm{Rh(dmpe)_2}]\mathrm{Cl} + \mathrm{Se_8} \xrightarrow[\mathrm{C_6H_6-THF}]{25\ ^\circ\mathrm{C},\ 12\ \mathrm{days}} \mathbf{7} \qquad (6)$$

1–**7** of Table II. In reaction 4 the initial product is an uncharacterized yellow-brown complex; the purple product **4** forms on prolonged standing. Reaction 6 also gives rise to significant amounts of an uncharacterized brown compound, but it is not known whether this is a precursor or coproduct of compound **7**.[53]

Complexes **1**–**7** are shown to be monomeric 1:1 electrolytes by conductivity measurements made in actonitrile and nitromethane solution as a function of concentration.[55,56] Plots of Λ vs. $c^{1/2}$ are linear over the range of measurement (10^{-2}–10^{-4} M). Table III summarizes the values of the intercept Λ_0 and the slope A. Also given in Table III are the theoretical slopes calculated from the Onsager relation[55] for a 1:1 electrolyte with the measured Λ_0.

The dppe complexes **1**, **2**, and **4** are readily soluble in dichloromethane and chloroform, soluble in acetonitrile, nitromethane, and alcohols, but insoluble in water, ether, THF, and benzene. The dmpe complexes **3**, **5**, **6**, and **7** have similar solubility properties, except that they decompose in chlorinated solvents and the chloride salts are soluble in water. Complexes **1**, **2**, **4**, and **6** are unchanged on exposure to air in the solid state, but the dmpe chloride salts **3**, **5**, and **7** are hygroscopic.

The disulfur complex **1** has been shown[6] to have a structure like that of the analogous dioxygen complex,[36] in which the Ir atom has cis-octahedral coordination and the S_2 ligand is

---

(50) D. T. Cromer and J. T. Waber, "International Tables for X-ray Crystallography", Vol. IV, Kynoch Press, Birmingham, England, 1974, Table 2.2B.

(51) D. T. Cromer, ref 50, Table 2.3.1.

(52) See paragraph at end of paper for details.

(53) The reaction of $[\mathrm{Ir(dmpe)_2}]\mathrm{Cl}$ with *cyclo*-octaselenium is not analogous to reactions 1–6. The major product is $[\mathrm{Ir(Se_4)(dmpe)_2}]\mathrm{Cl}$, with only small amounts of $[\mathrm{Ir(Se_2)(dmpe)_2}]\mathrm{Cl}$ being formed.[54]

(54) A. P. Ginsberg and C. R. Sprinkle, to be submitted for publication.

(55) P. Walden and E. J. Birr, *Z. Phys. Chem.* (*Leipzig*), **144**, 269 (1929).

(56) J. F. Coetzee and G. P. Cunningham, *J. Am. Chem. Soc.*, **87**, 2529 (1965).

bonded side-on (structure I). A similar coordination geometry, with side-on bonded Se_2, is demonstrated for compound **2** by the X-ray structure determination reported in this paper. Compounds **3–7** are inferred to have structure I from their conductivities and spectroscopic characterization (see below).

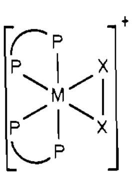

X = O, S, Se
M = Rh, Ir
I

Complexes **1** and **2** are extremely resistant to oxidation or substitution by O_2. No change was found when a dichloromethane solution of $[Ir(S_2)(dppe)_2]Cl$ was stirred under an oxygen atmosphere for 10 h or when the solid compound was heated for 52 h at 80 °C under and oxygen pressure of 650 atm. $[Ir(Se_2)(dppe)_2]Cl$ in acetonitrile solution was unchanged after being shaken for 3 days under 4 atm of oxygen (25 °C).

When a solution containing one of the disulfur or diselenium complexes **1–7** is stirred with metallic mercury, the sulfur or selenium is stripped from the complex (reaction 7). A similar, but very slow, reaction occurs with $[Ir(O_2)(dppe)_2]Cl$. The rate of reaction 7 varies greatly, depending on M, Y, and L–L. Table IV summarizes some measurements which indicate that the rate depends on M, Y, and L–L in the following manner:

$$[M(Y_2)(L\text{–}L)_2]^+ + 2Hg \xrightarrow[CH_3CN]{} [Ir(L\text{–}L)_2]^+ + 2HgY$$

L–L = dmpe, dppe; M = Rh, Ir; Y = O, S, Se (7)

$$Rh >> Ir \qquad dppe >> dmpe \qquad Se >> S \sim O$$

Tertiary phosphines abstract S and Se from the disulfur and diselenium complexes and form tertiary phosphine sulfides or selenides (e.g., reaction 8). This reaction is analogous to the well-known[34] oxidation of tertiary phosphines by dioxygen complexes. Other things being equal, the rate of the reaction is greater with an Se_2 than an S_2 complex and increases with increasing basicity of the phosphine. Thus, $PEtPh_2$ completely stripped the Se from $[Ir(Se_2)(dppe)_2]Cl$ after 17 h, but with PPh_3 only 85% of the Se had been abstracted after 4 days. In the case of $[Ir(S_2)(dppe)_2]Cl$ and $PEtPh_2$, reaction was evident after 24 h and was ca. 30% complete after 12 days. As previously reported, there is no evidence of reaction between $[Ir(S_2)(dppe)_2]Cl$ and PPh_3 after 24 h.[33]

$$[Ir(Se_2)(dppe)_2]^+ + 2PPh_3 \xrightarrow[CH_3CN]{} [Ir(dppe)_2]^+ + 2Ph_3PSe \quad (8)$$

Iodine reacts with compound **1** by adding 1 mol of I_2/mol of complex:

$$[Ir(S_2)(dppe)_2]Cl + I_2 \xrightarrow[CH_2Cl_2]{} \mathbf{17} \quad (9)$$

The product is a monomeric 1:1 electrolyte (Table III), which we believe to have the cis-octahedral structure II, analogous to $[Ir(SO)_2(dppe)_2]^+$.[31]

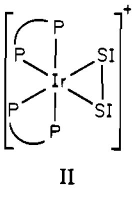

II

When compound **1** is reacted with $[Pt(PPh_3)_3]$ or $[Pt(PEtPh_2)_3]$ in 1:1 molar ratio, the platinum complex loses 1 mol of tertiary phosphine and adds to the disulfur complex (reactions 10 and 11). Similar addition reactions take place between the disulfur complex **5** and $[Pt(PPh_3)_3]$ and between the diselenium complex **2** and $[IrCl(CO)(PEt_2Ph)_2]$ (reactions 12 and 13). Compound **18**, the addition product of $[Pt(PPh_3)_3]$ with compound **1**, is unstable in solution (e.g., an ~1 mM solution in CH_3CN decomposed completely in about 2 h at room temperature under an He atmosphere), but compound **19**, the addition product with $Pt(PEtPh_2)_3$, is considerably more stable (an ~0.2 mM solution required about 50 h for complete decomposition). Acetonitrile solutions of the addition products **20** and **25** showed no change on overnight standing. Conductivity measurements (Table III) on products **19**, **20**, and **25** show them to be monomeric 1:1 electrolytes. These compounds presumably have the $(\mu\text{-}S)_2$ or $(\mu\text{-}Se)_2$ structures III and IV and reactions 10–13 are oxidative additions across the S–S or Se–Se bonds.

$$[Ir(S_2)(dppe)_2]Cl + [Pt(PPh_2R)_3] \xrightarrow[CH_3CN\text{-}THF\text{-}toluene]{R = Ph} \mathbf{18} \quad (10)$$

$$[Ir(S_2)(dppe)_2]Cl + [Pt(PPh_2R)_3] \xrightarrow[CH_3CN,\ NH_4PF_6]{R = Et} \mathbf{19} \quad (11)$$

$$[Rh(S_2)(dmpe)_2]Cl + [Pt(PPh_3)_3] \xrightarrow[CH_3CN\text{-}THF\text{-}toluene]{} \mathbf{20} \quad (12)$$

$$[Ir(Se_2)(dppe)_2]Cl + [IrCl(CO)(PEt_2Ph)_2] \xrightarrow[CH_2Cl_2]{} \mathbf{25} \quad (13)$$

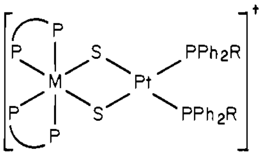

M = Rh, Ir
III

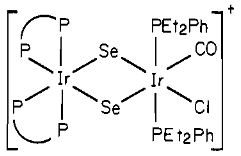

IV

Oxidative addition across the Se–Se bond in a diselenium complex takes place more readily than across the S–S bond in an isostructural disulfur complex. This is shown by the fact that, although $[IrCl(CO)(PEt_2Ph)_2]$ adds to compound **2**, it does not add to compound **1** under similar conditions. If the electron density at the added iridium is reduced by changing the phosphine from PEt_2Ph to PPh_3, addition across the Se–Se bond of compound **2** no longer occurs:

$$[Ir(Se_2)(dppe)_2]Cl + [IrCl(CO)(PPh_3)_2] \xrightarrow[CHCl_3]{} \text{no reaction}$$

We have been unable to make a mixed-metal $(\mu\text{-}Se)_2$ complex analogous to the $(\mu\text{-}S)_2$ Ir-Pt complexes **18** and **19** since $Pt(PPh_3)_3$ and $Pt(PEtPh_2)_{3,4}$ not only add across the Se–Se bond of compound **2** but also displace the Ir from Se (reactions 14 and 15). Product **24** undoubtedly has the diplatinum $(\mu\text{-}Se)_2$ structure V, analogous to known sulfur-bridged di-

$$[Ir(Se_2)(dppe)_2]BPh_4 + Pt(PPh_3)_3 \xrightarrow[CH_3CN\text{-}THF]{} \mathbf{23} + {}^1/_2[Ir(dppe)_2]BPh_4 + {}^1/_2[Ir(Se_2)(dppe)_2]BPh_4 \quad (14)$$

$$[Ir(Se_2)(dppe)_2]Cl + 2Pt(PEtPh_2)_4 \xrightarrow[CH_3CN]{} \mathbf{24} + [Ir(dppe)_2]Cl \quad (15)$$

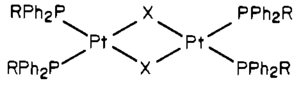

R = Et, Ph; X = S, Se
V

Table II. Analytical Data for Tertiary Phosphine Rhodium, Iridium, and Platinum Complexes with Sulfur and Selenium

no.	compd^a	color^b	mp, °C		anal.						mol wt
					% C	% H	% P	% S or Se	% halogen	% metal	
1	$[Ir(S_2)(dppe)_2]Cl$	s.y Pink	218-221	calcd	57.4	4.4	11.4	5.9	3.3		
				found	57.4	4.75	11.2	5.8	3.3		
2	$[Ir(Se_2)(dppe)_2]Cl$	d.y.G	200-201	calcd	52.8	4.1	10.5	13.4	3.0		
				found	52.9	4.5	10.1	13.0	3.1		
3	$[Ir(S_2)(dmpe)_2]Cl$	l.OY	249-253 dec	calcd	24.3	5.4	20.9	10.8	6.0		
				found	24.1	5.2	20.7	11.0	5.9		
4	$[Rh(S_2)(dppe)_2]Cl$	m.p	dec pt ~200	calcd	62.5	4.8	12.4	6.4	3.55		
				found	62.1	4.8	12.5	6.4	3.5		
5	$[Rh(S_2)(dmpe)_2]Cl$	l.yBr	154-155	calcd	28.7	6.4	24.6	12.8	7.05		
				found	28.5	6.4	24.4	12.9	7.2		
6	$[Rh(S_2)(dmpe)_2]PF_6$	OY	174-175	calcd	23.5	5.3	25.3	10.5			
				found	23.4	5.2	24.8	10.5			
7	$[Rh(Se_2)(dmpe)_2]Cl$	brill.yG	217-219 dec	calcd	24.2	5.4	20.8	26.5	5.9		
				found	24.3	5.5	20.5	26.3	6.05		
8	$[\{Ir(Se_2)Cl(CO)(PPh_3)\}_3]$	brO	dec pt ~240	calcd	33.8	2.2	4.6	23.4	5.25		2028
				found	33.5	2.3	4.6	23.2	5.1		2027,^{c} 2040^d
9	$[\{Ir(Se_2)Br(CO)(PPh_3)\}_3]$	brO	dec pt 230-240	calcd	31.7	2.1	4.3	21.9	11.1		2161
				found	31.3	2.1	4.3	22.2	10.8		1980^c
10	$[\{Ir(Se_2)Cl(CO)(AsPh_3)\}_3]$	l.Br	dec pt 235-240	calcd	31.7	2.1	10.4^e	21.9	4.9		2159
				found	32.0	2.3	10.3^e	21.8	4.8		2220^c
11	$[\{IrS_6Cl(CO)(PPh_3)_2\}_n]$	deep OY	149-150	calcd	45.7	3.1	6.4	19.8	3.6		
				found	45.9	3.4	6.0	19.8	3.2		
12	$[\{RhS_3Cl(PPh_3)\}_4]$	d.gy.yBr	dec pt >250	calcd	43.5	3.0	6.2	19.4	7.1		1987
				found	43.6	3.0	6.1	19.1	6.9		1700,^{c} 1860^d
13	$[\{RhS_3Br(PPh_3)\}_4]$	d.gy.yBr	dec pt >250	calcd	39.9	2.8	5.7	17.8	14.8		2165
				found	40.2	2.9	5.9	17.7	14.1		1940,^{c} 2040^d
14	$[\{RhSe_3Cl(PPh_3)\}_4]$	d.gy.Br	dec pt >250	calcd	33.9	2.4	4.9	37.2	5.6		2550
				found	34.15	2.4	4.7	37.2	5.6		2420^c
15	$[\{RhS_2Cl(AsPh_3)\}_n]$	d.yBr	dec pt ~230	calcd	42.5	3.0	14.7^e	12.6	7.0		1526 ($n = 3$) 2035 ($n = 4$) 2544 ($n = 5$)
				found	42.6	3.2	14.5^e	12.7	6.8		1320,^{c} 2020,^{d} 2460^d
16	$[\{RhSe_2Cl(AsPh_3)\}_n]$	d.Br	dec pt ~235	calcd	35.9	2.5	12.4^e	26.2	5.9		2410 ($n = 4$) 3013 ($n = 5$)
				found	36.1	2.4	12.7^e	25.8	6.1		2000,^{c} 3100^d
17	$[Ir(SI)_2(dppe)_2]Cl$	d.Red	dec pt 217-230	calcd	46.5	3.6	9.2	4.8	18.9,^{f} 2.6^g		
				found	46.2	3.6	9.3	4.7	19.1,^{f} 2.8^g		
18	$[(dppe)_2IrS_2Pt(PPh_3)_2]Cl$	m.OY	215-218 dec	calcd	58.45	4.35	10.3	3.55	2.0	10.6,^{h} 10.8^i	
				found	58.3	4.4	10.1	3.5	1.8	10.4,^{h} 10.6^i	
19	$[(dppe)_2IrS_2Pt(PEtPh_2)_2]PF_6$	l.OY	dec pt 141-147	calcd	52.7	4.3	3.5	11.9		10.55,^{h} 10.7^i	
				found	53.0	4.45	3.7	12.2		10.5,^{h} 10.6^i	
20	$[(dmpe)_2RhS_2Pt(PPh_3)_2]Cl$	s.Y	217-220 dec	calcd	47.2	5.1	15.2	5.25	2.9	16.0,^{i} 8.4^j	
				found	46.9	5.1	15.1	5.1	2.7	15.7,^{i} 8.4^j	
21	$[\{PtS(PPh_3)_2\}_n]$	OY	280-282 dec	calcd	57.5	4.0	8.2	4.3		26.0	
				found	57.6	4.2	8.4	4.6		25.6	
22	$[\{PtS(PEtPh_2)_2\}_2]$	s.O	188-189	calcd	51.3	4.6	9.45	4.9		29.8	1311
				found	51.4	4.5	9.5	5.4		29.5	1222^k
23	$[\{PtSe(PPh_3)_2\}_n]\cdot nC_4H_8O$	yBr	280-281 dec	calcd	55.2	4.4	7.1	9.1			
				found	55.2	4.5	7.3	8.5			
24	$[\{PtSe(PEtPh_2)_2\}_2]\cdot C_7H_{16}$	deep rO	190^l	calcd	50.3	5.1	8.2	10.5		25.9	1405^m
				found	50.4	5.1	8.4	10.4		25.5	1430^k
25	$[(dppe)_2IrSe_2IrCl(CO)(PEt_2Ph)_2]Cl$	OY		calcd	49.5	4.4	10.5	8.9	4.0	21.7	
				found	49.4	4.5	10.3	8.8	4.2	21.6	
26	$[\{IrSeCl(CO)(PEt_2Ph)_2\}_2]$	s.O	165-166	calcd	37.8	4.5	9.3	11.8			1334
				found	37.7	4.5	9.4	12.0			1277^c

[a] dppe = $(C_6H_5)_2PCH_2CH_2P(C_6H_5)_2$, dmpe = $(CH_3)_2PCH_2CH_2P(CH_3)_2$, Ph = C_6H_5. [b] ISCC-NBS color names. [c] In chloroform. [d] In benzene. [e] % As. [f] % I. [g] % Cl. [h] % Ir. [i] % Pt. [j] % Rh. [k] In toluene. [l] Solvent of crystallization is lost at 70-78 °C. [m] Without the heptane of crystallization.

platinum complexes.[57] Product **23** was too insoluble[58] for molecular weight determination but presumably has the same structure. A complex with essentially the same stoichiometry and color as those of compound **23** has been isolated from the

---

(57) J. Chatt and D. M. P. Mingos, *J. Chem. Soc. A*, 1243 (1970).

(58) Compounds **21** and **23** dissolve in $CHCl_3$ but appear to react with this solvent.

Table III. Conductivity Data for Ionic Complexes[a]

no.	compd	Λ_0, Ω^{-1} cm^2	A- (obsd)	A- (theory, 1:1)
1	$[Ir(S_2)(dppe)_2]Cl$	139	380	333
2	$[Ir(Se_2)(dppe)_2]Cl$	125	329	322
3	$[Ir(S_2)(dmpe)_2]Cl$	136	334	330
4	$[Rh(S_2)(dppe)_2]Cl^b$	85	160	191
6	$[Rh(S_2)(dmpe)_2]PF_6$	160	365	349
7	$[Rh(Se_2)(dmpe)_2]Cl$	157	412	346
17	$[Ir(SI)_2(dppe)_2]Cl^c$	27	69	65
19	$[(dppe)_2IrS_2Pt(PEtPh_2)_2]PF_6$	158	410	347
20	$[(dmpe)_2RhS_2Pt(PPh_3)_2]Cl$	139	316	332
25	$[(dppe)_2IrSe_2IrCl(CO)(PEt_2Ph)_2]Cl^d$	185	458	367

[a] Measurements in acetonitrile solution at 25 °C unless otherwise indicated. All plots of Λ_e vs. $c^{1/2}$ were linear. [b] In nitromethane solution. For comparison, $[Ir(S_2)(dppe)_2]Cl$ in nitromethane solution gives $\Lambda_0 = 83$ and $A = 167$ (A(theory, 1:1) = 190). [c] In nitrobenzene solution. [d] The sample recovered after the conductivity measurement was unchanged in its CO stretching frequency.

Table IV. Percent Conversion of $[M(X_2)(L\text{-}L)_2]Cl$ to $[M(L\text{-}L)_2]Cl$ on Stirring with Mercury in Acetonitrile at 25 °C[a]

		% conversion after stirring	
no.	compd	2 h	10 days
	$[Ir(O_2)(dppe)_2]Cl$		~2%
1	$[Ir(S_2)(dppe)_2]Cl$		small amt[c]
2	$[Ir(Se_2)(dppe)_2]Cl$	100	
4	$[Rh(S_2)(dppe)_2]Cl$	100[b]	
5	$[Rh(S_2)(dmpe)_2]Cl$		small amt[c]
6	$[Rh(Se_2)(dmpe)_2]Cl$	100	

[a] 10–20 mL of a (2–3) × 10^{-3} M solution was vigorously stirred with approximately 0.5 g of Hg under an He atmosphere. [b] In a repeat experiment 4 h was required for complete conversion. [c] A small amount of black HgS formed, but the percent conversion could not be determined from the optical spectrum.

reaction of $Pt(PPh_3)_3$ and S_8 and proposed to have structure V.[59] A diiridium $(\mu\text{-}Se)_2$ complex, structure VI, is obtained if reaction 13 is carried out in acetonitrile with 2 mol of $[IrCl(CO)(PEt_2Ph)_2]$/mol of the diselenium complex:

$$[Ir(Se_2)(dppe)2]Cl + 2[IrCl(CO)(PEt_2Ph)_2] \xrightarrow[CH_3CN]{} \mathbf{26} \qquad (16)$$

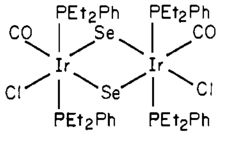

VI

Analogous sulfur-bridged iridium complexes do not appear to be known. Known[57,59] diplatinum $(\mu\text{-}S)_2$ complexes with structure V are formed when reactions 10 and 11 are carried out in acetonitrile with a 2:1 molar ratio of Pt to Ir complex (reaction 17).

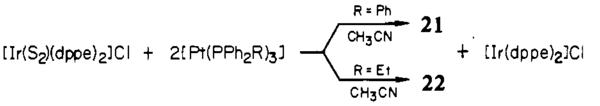

$$[Ir(S_2)(dppe)_2]Cl + 2[Pt(PPh_2R)_3] \begin{cases} \xrightarrow[CH_3CN]{R = Ph} \mathbf{21} \\ \xrightarrow[CH_3CN]{R = Et} \mathbf{22} \end{cases} + [Ir(dppe)_2]Cl \qquad (17)$$

Oxidative addition reactions of the type (10)–(17) have not been reported for dioxygen complexes, and we have found no evidence of reaction when $[Ir(O_2)(dppe)_2]Cl$ is mixed with $Pt(PPh_3)_3$ or $Pt(PPh_2Et)_3$ in acetonitrile or methylene chloride solution. Our results indicate that, for isostructural $[M(Y_2)(L\text{-}L)_2]^+$ complexes, the ability to undergo oxidative addition of a low-valent group 8 metal complex across the Y–Y bond decreases in the order Y = Se > S >> O.

Vaska's compound, $IrCl(CO)(PPh_3)_2$, has been reported[59] to react with *cyclo*-octasulfur, forming a brick red material of formula $[\{IrS_2Cl(CO)(PPh_3)\}_3]$. In our hands the reaction was

$$[IrCl(CO)(PPh_3)_2] + S_8 \xrightarrow[C_6H_6]{} \mathbf{11} + \text{other products} \qquad (18)$$

"Other Products" refers to a mixture of benzene- and chloroform-soluble compounds, which we could not characterize. Product **11** was too insoluble for molecular weight determination. Reactions with *cyclo*-octaselenium, on the other hand, gave characterizable soluble products analogous to the reported[59] sulfur complex. Thus, we found

$$[IrX(CO)(PPh_3)_2] + Se_8 \xrightarrow[C_6H_6]{50\text{–}60\ °C} \mathbf{8}\ (X = Cl),\ \mathbf{9}\ (X = Br) \qquad (19)$$

and

$$[IrCl(CO)(AsPh_3)_2] + Se_8 \xrightarrow[C_6H_6]{} \mathbf{10} \qquad (20)$$

Products **8**–**10** are soluble in benzene, chloroform, tetrahydrofuran, and acetone but insoluble in ether and hexane. Osmometric molecular weight measurements in both benzene and chloroform (Table II) show them to be trimeric. The mass spectrum[60] of compound **8** at 200 °C is essentially that of Ph_3P with a small amount of Ph_3PS; the latter is presumably formed by reaction in the spectrometer source. There are no peaks attributable to metal-containing fragments.

Oligomeric complexes containing sulfur and selenium are also obtained from the reaction between $[RhX(PPh_3)_3]$ (X = Cl, Br) or $[RhCl(AsPh_3)_3]$ and *cyclo*-octasulfur or *cyclo*-octaselenium (reactions 21–24). Products **12**–**16** are soluble in chloroform and benzene. Osmometric molecular weight measurements (Table II) indicate that compounds **12**–**14** are close to tetrametric in chloroform and benzene solution. Compounds **15** and **16**, however, gave variable molecular weight results, indicating that their degree of association depends on the solvent and concentration. The Ph_3P complex **12**, with S:Rh = 3, is converted to the Ph_3As complex **15**, with S:Rh = 2, by reaction with excess Ph_3As in boiling benzene. Treatment of compound **12** with excess Ph_3P in refluxing benzene leads to sulfur abstraction and a product of approximate composition $RhSCl(PPh_3)$.

$$[RhX(PPh_3)_3] + S_8 \xrightarrow[C_6H_6]{} \mathbf{12}\ (X = Cl),\ \mathbf{13}\ (X = Br) \qquad (21)$$

$$[RhCl(PPh_3)_3] + Se_8 \xrightarrow[C_6H_6]{60\text{–}70\ °C} \mathbf{14} \qquad (22)$$

$$[RhCl(AsPh_3)_3] + S_8 \xrightarrow[C_6H_6]{} \mathbf{15} \qquad (23)$$

$$[RhCl(AsPh_3)_3] + Se_8 \xrightarrow[C_6H_6]{60\text{–}70\ °C} \mathbf{16} \qquad (24)$$

Crystal Structure of $[Ir(Se_2)(dppe)_2]Cl\cdot H_2O\cdot 0.5C_6H_6$. The crystal structure consists of discrete $[Ir(Se_2)(dppe)_2]^+$ cations, Cl^- anions, and lattice H_2O and C_6H_6. There are 8 formula units per unit cell. Table V lists the final positional parameters (thermal parameters may be found in a supplementary table[52]), and Table VI gives the root-mean-square amplitudes of thermal vibration. Figure 1 is a perspective drawing of the $[Ir(Se_2)(dppe)_2]^+$ cation, which shows the atom numbering scheme. In Figure 2 the structure is shown without the phenyl rings, exhibiting the inner coordination sphere and dppe chelate rings. Tables VII and VIII summarize the bond distances and

---

(59) R. Ugo, G. LaMonica, S. Cenini, and F. Conti, *J. Chem. Soc. A*, 522 (1971).

(60) Mass spectra were measured by the Gollob Analytical Service Corp. using the direct-solids probe of a CEC 21-104 mass spectrometer.

Table V. Positional Parameters and Their Estimated Standard Deviations

atom	*x*	*y*	*z*
Ir	0.11686 (4)	0.10458 (7)	0.09778 (2)
Se1	0.0455 (1)	0.1104 (2)	0.03690 (4)
Se2	0.1276 (1)	0.2421 (2)	0.05384 (5)
Cl1	0.3508 (3)	0.2493 (6)	0.6686 (2)
P1	0.0573 (3)	−0.0222 (4)	0.1211 (1)
P2	0.0402 (3)	0.2302 (4)	0.1129 (1)
P3	0.1918 (3)	−0.0062 (4)	0.0766 (1)
P4	0.2100 (3)	0.1258 (4)	0.1447 (1)
O1	0.455 (1)	0.404 (2)	0.7143 (5)
C1	−0.0196 (9)	0.043 (2)	0.1288 (5)
C2	−0.0049 (9)	0.160 (2)	0.1416 (4)
C3	0.2779 (10)	0.006 (2)	0.1057 (5)
C4	0.2715 (10)	0.018 (2)	0.1433 (5)
C5	0.0133 (9)	−0.136 (1)	0.0971 (4)
C6	0.0184 (10)	−0.242 (2)	0.1126 (5)
C7	−0.0238 (12)	−0.322 (2)	0.0943 (6)
C8	−0.0696 (12)	−0.305 (2)	0.0609 (6)
C9	−0.0731 (11)	−0.201 (2)	0.0481 (5)
C10	−0.0328 (10)	−0.116 (2)	0.0650 (5)
C11	0.0985 (9)	−0.083 (2)	0.1615 (5)
C12	0.1527 (9)	−0.150 (2)	0.1626 (5)
C13	0.1872 (10)	−0.205 (2)	0.1927 (5)
C14	0.1600 (11)	−0.193 (2)	0.2210 (5)
C15	0.1056 (10)	−0.127 (2)	0.2204 (5)
C16	0.0737 (10)	−0.069 (2)	0.1912 (5)
C17	−0.0284 (9)	0.284 (2)	0.0794 (4)
C18	−0.0158 (10)	0.372 (2)	0.0614 (5)
C19	−0.0700 (12)	0.418 (2)	0.0337 (6)
C20	−0.1342 (11)	0.376 (2)	0.0290 (5)
C21	−0.1456 (11)	0.290 (2)	0.0479 (6)
C22	−0.0937 (10)	0.244 (2)	0.0744 (5)
C23	0.0708 (10)	0.353 (2)	0.1371 (5)
C24	0.1265 (11)	0.405 (2)	0.1316 (5)
C25	0.1461 (12)	0.508 (2)	0.1505 (6)
C26	0.1102 (12)	0.542 (2)	0.1725 (6)
C27	0.0529 (13)	0.495 (2)	0.1760 (6)
C28	0.0287 (11)	0.393 (2)	0.1578 (6)
C29	0.1749 (9)	−0.153 (2)	0.0734 (5)
C30	0.2241 (10)	−0.222 (2)	0.0932 (5)
C31	0.2063 (12)	−0.334 (2)	0.0875 (6)
C32	0.1462 (13)	−0.367 (2)	0.0664 (6)
C33	0.0993 (11)	−0.300 (2)	0.0485 (5)
C34	0.1126 (10)	−0.183 (2)	0.0518 (5)
C35	0.2102 (10)	0.022 (2)	0.0353 (5)
C36	0.1808 (9)	−0.038 (2)	0.0050 (5)
C37	0.1985 (11)	−0.018 (2)	−0.0246 (5)
C38	0.2431 (10)	0.065 (2)	−0.0268 (5)
C39	0.2714 (10)	0.122 (2)	0.0017 (5)
C40	0.2541 (9)	0.104 (2)	0.0322 (4)
C41	0.2614 (8)	0.248 (1)	0.1477 (4)
C42	0.2871 (10)	0.297 (2)	0.1780 (5)
C43	0.3227 (11)	0.397 (2)	0.1794 (5)
C44	0.3344 (11)	0.443 (2)	0.1500 (6)
C45	0.3129 (11)	0.390 (2)	0.1191 (5)
C46	0.2773 (10)	0.290 (2)	0.1174 (5)
C47	0.2025 (10)	0.120 (2)	0.1889 (5)
C48	0.1595 (10)	0.191 (2)	0.1986 (5)
C49	0.1583 (10)	0.188 (2)	0.2351 (5)
C50	0.1982 (11)	0.119 (2)	0.2568 (5)
C51	0.2410 (11)	0.047 (2)	0.2472 (6)
C52	0.2438 (11)	0.044 (2)	0.2115 (5)
C101	0.0000 (0)	0.637 (4)	0.2500 (0)
C102	0.0603 (15)	0.582 (3)	0.2679 (8)
C103	0.0624 (18)	0.462 (3)	0.2695 (9)
C104	0.0000 (0)	0.405 (4)	0.2500 (0)

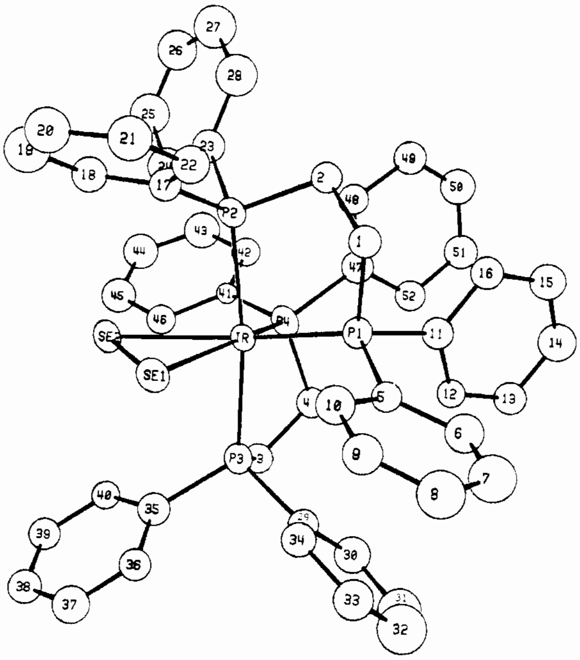

Figure 1. Perspective view of the $[Ir(Se_2)(dppe)_2]^+$ complex cation showing the atom numbering scheme. Thermal motion is represented by 50% probability ellipsoids or spheres.

Table VI. Root-Mean-Square Amplitudes of Thermal Vibration in Angstroms

atom	min	intermed	max
Ir	0.138	0.153	0.168
Se1	0.154	0.195	0.205
Se2	0.154	0.193	0.209
P1	0.158	0.168	0.181
P2	0.157	0.179	0.192
P3	0.144	0.183	0.186
P4	0.137	0.171	0.206
Cl1	0.231	0.260	0.321

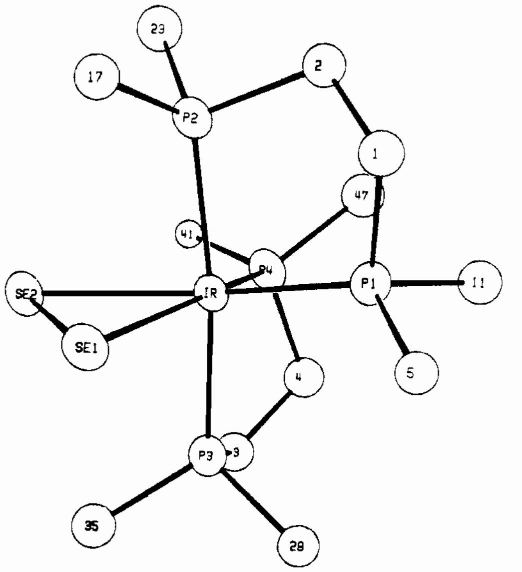

Figure 2. $[Ir(Se_2)(dppe)_2]^+$ inner coordination sphere and dppe chelate rings.

angles in the cation and in the lattice benzene molecule. Table IX describes certain significant planes in the structure.

$[Ir(Se_2)(dppe)_2]^+$ is similar in structure to its dioxygen and disulfur analogues; Table X presents a comparison of bond distances and angles in the three compounds and in $[Ir(S_2O_2)(dppe)_2]Cl$. The inner coordination geometry about the iridium atom is distorted cis-octahedral, with the Se_2 group bonded side-on to the iridium at equatorial positions and each dppe group chelating axial and equatorial positions. A 14.0° twist of the Ir–Se1–Se2 plane with respect to the Ir–P1–P4 plane (compare a 12.8° twist in the S_2 complex) reduces the

Table VII. Bond Distances in Angstroms[a]

atom 1	atom 2	dist	atom 1	atom 2	dist	atom 1	atom 2	dist
Ir	Se1	2.539 (2)	C9	C10	1.41 (3)	C35	C40	1.38 (2)
Ir	Se2	2.529 (2)	C11	C12	1.37 (2)	C36	C37	1.36 (2)
Ir	P1	2.327 (5)	C11	C16	1.43 (3)	C37	C38	1.39 (3)
Ir	P2	2.388 (5)	C12	C13	1.42 (2)	C38	C39	1.36 (2)
Ir	P3	2.365 (5)	C13	C14	1.41 (3)	C39	C40	1.39 (2)
Ir	P4	2.337 (5)	C14	C15	1.36 (3)	C41	C42	1.36 (2)
Se1	Se2	2.312 (3)	C15	C16	1.41 (3)	C41	C46	1.45 (2)
P1	C1	1.85 (2)	C17	C18	1.38 (2)	C42	C43	1.43 (3)
P1	C5	1.83 (2)	C17	C22	1.38 (2)	C43	C44	1.40 (3)
P1	C11	1.81 (2)	C18	C19	1.48 (3)	C44	C45	1.39 (3)
P2	C2	1.87 (2)	C19	C20	1.37 (3)	C45	C46	1.43 (3)
P2	C17	1.81 (2)	C20	C21	1.37 (3)	C47	C48	1.37 (2)
P2	C23	1.84 (2)	C21	C22	1.42 (3)	C47	C52	1.43 (3)
P3	C3	1.85 (2)	C23	C24	1.36 (3)	C48	C49	1.49 (2)
P3	C29	1.86 (2)	C23	C28	1.43 (3)	C49	C50	1.35 (3)
P3	C35	1.84 (2)	C24	C25	1.50 (3)	C50	C51	1.37 (3)
P4	C4	1.84 (2)	C25	C26	1.36 (3)	C51	C52	1.47 (3)
P4	C41	1.83 (2)	C26	C27	1.34 (3)	C101	C102	1.43 (3)
P4	C47	1.85 (2)	C27	C28	1.49 (3)			
C1	C2	1.55 (2)	C29	C30	1.41 (3)	C102	C103	1.51 (4)
C3	C4	1.58 (2)	C29	C34	1.39 (2)	C103	C104	1.49 (4)
C5	C6	1.45 (3)	C30	C31	1.45 (3)			
C5	C10	1.43 (2)	C31	C32	1.36 (3)	Cl1	O1	3.10 (2)
C6	C7	1.40 (3)	C32	C33	1.33 (3)	O1	O1	3.03 (4)
C7	C8	1.46 (3)	C33	C34	1.48 (3)			
C8	C9	1.40 (3)	C35	C36	1.44 (3)			

[a] Numbers in parentheses are estimated standard deviations in the least significant digits.

local symmetry to C_2. Both dppe chelate rings are puckered, having the ethylenic carbon atoms on opposite sides of the Ir–P–P plane, but it is evident from Table IX that the rings are substantially different. In the Ir–P1–C1–C2–P2 ring C1 and C2 are equidistant from the Ir–P1–P2 plane, while in the Ir–P3–C3–C4–P4 ring C4 is more than twice as far as C3 from the Ir–P3–P4 plane. Similarly puckered and nonequivalent dppe chelate rings have been described for the disulfur complex.[6]

Compared to the free Se_2 molecule (Se–Se distance 2.19 (3) Å[61]), the iridium-bonded Se_2 group has a 0.16 Å longer Se–Se bond, very close to the bond length in Se_8 (2.336 (6) Å[62]). Similar bond lengthening has been observed in both $[Ir(O_2)(dppe)_2]^+$ and $[Ir(S_2)(dppe)_2]^+$. In the dioxygen complex the O–O distance is slightly greater than the bond length in O_2^{2-} (1.49 Å), while in the disulfur complex the S–S distance is slightly less than the bond length in S_2^{2-} (2.08 Å in SrS_2, 2.13 Å in Na_2S_2); the bound O_2 and S_2 groups therefore have bond orders close to 1. Although the Se–Se distance in Se_2^{2-} is not available for comparison, the close similarity between S–S and Se–Se bond lengthening in the complexes suggests that the bound Se_2 group also has a bond order of about 1. The Se–Se distance in $[Ir(Se_2)(dppe)_2]^+$ is very close to the value found for bridging Se_2 in $Fe_2(CO)_6(\mu\text{-}Se_2)$ (2.293 (2) Å)[20] and for the terminal side-on Se_2 group in $Os(Se_2)(CO)_2(PPh_3)_2$ (2.321 (1) Å).[21]

In iridium diselenide, the only compound for which an Ir–Se distance has been reported,[63] an iridium atom in the +3 oxidation state is octahedrally coordinated by six selenium atoms, three at a distance of 2.52 Å and three at 2.44 Å. The longer of these distances is very close to the value found in $[Ir(Se_2)(dppe)_2]^+$.

The Ir–P distances found for the diselenium complex are very similar to the values found for the related compounds in Table X. Like the other compounds, $[Ir(Se_2)(dppe)_2]^+$ has longer axial than equatorial Ir–P bonds. The average $P–C_{phenyl}$ distances in the O_2, S_2, and Se_2 complexes are essentially the same.

Vibrational Spectra. Table XI presents the frequencies of selected vibrations in compounds **1–26**. These assignments were made by intercomparison of the spectra of related compounds.

In the dmpe disulfur complexes **3**, **5**, and **6**, the ν(S–S) frequency occurs in a region free of ligand absorption and may be assigned with confidence by comparison with the spectrum of the Se_2 complex **7**. However, in the dppe disulfur complexes **1** and **4**, ν(S–S) occurs in the same region as the dppe X-sensitive modes,[64,65] and it could not be certainly identified. Bands at 545 cm^{-1} (sh) in **1**,[66] 550 cm^{-1} (w) in **4**, and 548 cm^{-1} in the I_2 adduct **17** are tentatively assigned as ν(S–S) in Table XI. However, against this assignment we note that although $[Ir(Se_2)(dppe)_2]Cl$ does not have a corresponding band in its vibrational spectrum, such a band is present (unassigned) in the spectra of free dppe and of PPh_3 (540 cm^{-1})[64,65] and is at 554 cm^{-1} in the spectrum of $[Ir(O_2)(dppe)_2]Cl$.

The ν(S–S) frequencies in Table XI are less than the values for the free S_2 molecule (718 cm^{-1})[67] and the S_2^- ion (610 cm^{-1} in NaBr host, 592 cm^{-1} in NaI host)[68] but greater than the value for the S_2^{2-} ion (446 cm^{-1} in Na_2S_2).[30] They are similar to the values for ν(S–S) in other complexes containing side-on bonded S_2, e.g., 540 cm^{-1} in $(\pi\text{-}C_5H_5)_2NbS_2X$ (X = Cl, Br, I, SCN)[3] and 530 cm^{-1} in $[Mo_2(S_2)_6]^{2-}$.[30] In contrast, ν(O–O) for side-on bonded O_2 (800–900 cm^{-1})[69] is *less* than the value for the peroxide ion (1081 cm^{-1} in Na_2O_2).

An Se–Se stretching frequency is identified for compounds **2** and **7** in Table XI; the values are close to the reported ν(Se–Se) of side-on Se_2 in $[Os(Se_2)(CO)_2(PPh_3)_2]$ (312 cm^{-1}) and $[Os(Se_2)(CO)(CNC_7H_7)(PPh_3)_2]$ (309 cm^{-1}).[21] These frequencies are about 5% less than in the Se_2^- ion (325 cm^{-1} in KI host).[68] This is similar to an 8% decrease in ν(S–S) for side-on bonded S_2 compared to that for the S_2^- ion.

Attempts were made to identify S–S and Se–Se stretching frequencies for other compounds in Table II, where the formula suggests the presence of an S_x or Se_x group. Comparison of the spectra of compounds **15** and **16** reveals a Raman shoulder at 510 cm^{-1} (IR, 507 cm^{-1}) in compound **15** but not in **16**; we tentatively assign this as an S_2 group ν(S–S) frequency. The corresponding ν(Se–Se) frequency in compound **16** may be associated with a Raman shoulder at ~285 cm^{-1}. Intercomparison of the IR spectra of compounds **8–11** gave no evidence of a ν(S–S) or ν(Se–Se) frequency. The Raman spectra of compounds **8–10** could not be obtained, but compound **11** gave a good spectrum. A strong band at 487 cm^{-1} in this spectrum is not present in the Raman spectrum of $[IrCl(CO)(PPh_3)_2]$ and is presumably due to ν(S–S) of an S_x group. We also failed to obtain Raman spectra of compounds **12–14**, and the IR spectra gave no evidence of bands attributable to S–S or Se–Se stretching modes. Failure to identify ν(S–S) or ν(Se–Se) frequencies in the IR spectra of compounds **8–10** and **12–14** is not significant since the regions in which

---

(61) L. R. Maxwell and V. M. Mosley, *Phys. Rev.*, **57**, 21 (1940).

(62) P. Cherin and P. Unger, *Acta Crystallogr., Sect. B*, **B28**, 313 (1972).

(63) L. B. Barricelli, *Acta Crystallogr.*, **11**, 75 (1958).

(64) M. Bacci, *Spectrochim. Acta, Ser. A*, **28A**, 2286 (1972).

(65) G. B. Deacon and J. H. S. Green, *Spectrochim. Acta, Ser. A*, **24A**, 845 (1968).

(66) Compound 1 exists in two crystalline forms, prisms and plates. The 545-cm^{-1} band occurs in the solid-state Raman and IR spectra of the plate form but not of the prism form. Raman spectra of nitromethane solutions of either form have a strongly polarized band at 542 cm^{-1}. A possible explanation of this behavior is that the weak ortho phenyl hydrogen–sulfur interaction that exists in this compound (see section on NMR spectra) is different in the two crystalline forms and that this causes the 542-cm^{-1} band to shift enough in the prism form so that it is blocked by the nearby ligand band.

(67) K. K. Yee, R. F. Barrow, and A. Rogstad, *J. Chem. Soc., Faraday Trans. 2*, **68**, 1808 (1972).

(68) W. Holzer, W. F. Murphy, and H. J. Bernstein, *J. Mol. Spectrosc.*, **32**, 13 (1969).

(69) L. Vaska, *Acc. Chem. Res.*, **9**, 175 (1976).

Table VIII. Bond Angles in Degrees[a]

atom 1	atom 2	atom 3	angle	atom 1	atom 2	atom 3	angle	atom 1	atom 2	atom 3	angle
Se1	Ir	Se2	54.28 (7)	C4	P4	C41	103.5 (8)	C23	C28	C27	115 (2)
Se1	Ir	P1	101.2 (1)	C4	P4	C47	102.8 (9)	P3	C29	C30	118 (1)
Se1	Ir	P2	89.4 (1)	C41	P4	C47	98.7 (8)	P3	C29	C34	115 (1)
Se1	Ir	P3	85.2 (1)	P1	C1	C2	112 (1)	C30	C29	C34	126 (2)
Se1	Ir	P4	160.0 (1)	P2	C2	C1	108 (1)	C29	C30	C31	113 (2)
Se2	Ir	P1	153.5 (1)	P3	C3	C4	110 (1)	C30	C31	C32	122 (2)
Se2	Ir	P2	85.0 (1)	P4	C4	C3	109 (1)	C31	C32	C33	124 (2)
Se2	Ir	P3	87.8 (1)	P1	C5	C6	120 (1)	C32	C33	C34	119 (2)
Se2	Ir	P4	108.0 (1)	P1	C5	C10	118 (1)	C29	C34	C33	116 (2)
P1	Ir	P2	84.7 (2)	C6	C5	C10	121 (2)	P3	C35	C36	124 (2)
P1	Ir	P3	101.2 (2)	C5	C6	C7	117 (2)	P3	C35	C40	120 (1)
P1	Ir	P4	97.7 (2)	C6	C7	C8	124 (2)	C36	C35	C40	116 (2)
P2	Ir	P3	172.7 (2)	C7	C8	C9	116 (2)	C35	C36	C37	122 (2)
P2	Ir	P4	98.8 (2)	C8	C9	C10	123 (2)	C36	C37	C38	121 (2)
P3	Ir	P4	84.8 (2)	C5	C10	C9	118 (2)	C37	C38	C39	118 (2)
Ir	Se1	Se2	62.63 (7)	P1	C11	C12	118 (1)	C38	C39	C40	122 (2)
Ir	Se2	Se1	63.09 (7)	P1	C11	C16	122 (1)	C35	C40	C39	121 (2)
Ir	P1	C1	108.0 (6)	C12	C11	C16	119 (2)	P4	C41	C42	121 (1)
Ir	P1	C5	122.8 (6)	C11	C12	C13	123 (2)	P4	C41	C46	119 (1)
Ir	P1	C11	119.3 (6)	C12	C13	C14	117 (2)	C42	C41	C46	119 (2)
C1	P1	C5	96.9 (8)	C13	C14	C15	122 (2)	C41	C42	C43	120 (2)
C1	P1	C11	104.2 (8)	C14	C15	C16	121 (2)	C42	C43	C44	121 (2)
C5	P1	C11	102.1 (8)	C11	C16	C15	118 (2)	C43	C44	C45	120 (2)
Ir	P2	C2	107.5 (6)	P2	C17	C18	119 (1)	C44	C45	C46	120 (2)
Ir	P2	C17	118.0 (6)	P2	C17	C22	120 (1)	C41	C46	C45	119 (2)
Ir	P2	C23	122.1 (6)	C18	C17	C22	121 (2)	P4	C47	C48	118 (1)
C2	P2	C17	104.4 (8)	C17	C18	C19	121 (2)	P4	C47	C52	119 (1)
C2	P2	C23	101.9 (8)	C18	C19	C20	117 (2)	C48	C47	C52	124 (2)
C17	P2	C23	100.6 (8)	C19	C20	C21	121 (2)	C47	C48	C49	116 (2)
Ir	P3	C3	107.6 (6)	C20	C21	C22	123 (2)	C48	C49	C50	121 (2)
Ir	P3	C29	118.5 (6)	C17	C22	C21	117 (2)	C49	C50	C51	123 (2)
Ir	P3	C35	121.1 (6)	P2	C23	C24	119 (2)	C50	C51	C52	118 (2)
C3	P3	C29	104.5 (8)	P2	C23	C28	116 (2)	C47	C52	C51	118 (2)
C3	P3	C35	101.5 (8)	C24	C23	C28	124 (2)	C102	C101	C102	122 (4)
C29	P3	C35	101.4 (9)	C23	C24	C25	116 (2)	C101	C102	C103	121 (3)
Ir	P4	C4	107.5 (6)	C24	C25	C26	120 (2)	C102	C103	C104	116 (4)
Ir	P4	C41	118.4 (5)	C25	C26	C27	123 (2)	C103	C104	C103	123 (5)
Ir	P4	C47	123.3 (6)	C26	C27	C28	121 (2)	Cl1	O1	O1	137.0 (5)

[a] Numbers in parentheses are estimated standard deviations in the least significant digits.

these vibrations are expected are densely populated by PPh_3 or $AsPh_3$ bands.

M–S and M–Se stretching frequencies have been identified for the $[M(X_2)(L\text{–}L)_2]^+$ complexes **1–7** and for the I_2 adduct **17**; the bands are very weak in the IR spectra but strong in the Raman spectra. Two Raman-active ν(M–S) or ν(M–Se) modes are expected for each of these compounds, but except for compounds **3** and **17**, only one is observed. Raman measurements on solutions of compound **1** show the ν(M–S) band to be strongly polarized, indicating that it is due to the A mode. In the solid state, the M–S stretching frequency of compound **1** occurs at 310 cm^{-1} in the plate form and at 300 cm^{-1} in the prism form. Table XI also contains assignments for ν(M–S) in compounds **11–13**, **15**, and **19**. Again only one band is observed except for compound **19** where the two bands expected for a $(\mu\text{-}S)_2$ structure are seen in the Raman spectrum. Attempts to observe M–S and M–Se stretching frequencies in compounds **20**, **25**, and **26** were prevented by phosphine ligand band interference.

Bands attributable to metal–halogen stretching vibraitons were detected in the spectra of compounds **8–16** (Table XI). A very strong band at 218 cm^{-1} in the Raman spectrum of **17** is reasonably assigned as a ν(S–I) frequency.

All of the CO-containing compounds in Table II have a single IR-active CO stretching frequency which is 70–100 cm^{-1} higher in energy than in the $IrX(CO)L_2$ complexes from which they are derived. This shows them to be oxidized adducts of the parent complex.

NMR Spectra. Six-coordinate $(dppe)_2$ complexes with cis geometry have characteristic ^1H NMR spectra, which may be used to establish the stereochemistry in uncertain cases.[70] The characteristic feature of the spectra results from the resonance of four ortho phenyl hydrogen atoms being shifted upfield from the main phenyl multiplet by interaction with the two non-phosphorus cis groups. The resonance is observed as a 1:2:1 triplet of intensity 4 protons if the cis groups are equivalent or as two triplets, each of intensity 2 protons, if the cis groups are nonequivalent.[70]

Table XII shows the results of ^1H NMR measurements on compounds **4**, **17**, and **19**; also shown are the previously published results for compounds **1** and **2**.[70a] All of these compounds show an ortho phenyl hydrogen triplet of intensity 4 protons at τ 3.6–3.9. These results establish cis-octahedral coordination with equivalent cis groups for the Rh atom in compound **4** and for the Ir atoms in compounds **17** and **19**.

Electronic Spectra. Figures 3 and 4 and Table XIII show the electronic absorption spectra of compounds **1**, **2**, **4**, and **7** in CH_3CN solution over the range 180–800 nm. Strong phenyl ring absorption in the dppe complexes prevents observation of transitions originating in the $[M(X_2)P_4]^+$ core of the complex below about 250 nm. Free dppe has its lowest energy phenyl ring absorption at 252 nm (ϵ 1.68 × 10^4 M^{-1} cm^{-1}); a band weakly red shifted with respect to this is expected in the complexes (cf. Ph_3PO with respect to Ph_3P[71]). Hence the highest energy feature (255–260 nm) observed for the dppe complexes is probably, at least in part, due to a dppe $\pi \rightarrow \pi^*$

---

(70) (a) A. P. Ginsberg and W. E. Lindsell, *Inorg. Chem.*, **12**, 1983 (1973). (b) See also J. Chatt, A. J. L. Pombeiro, and R. L. Richards, *J. Organomet. Chem.*, **184**, 357 (1980). Another example may be found in ref 28.

(71) H. H. Jaffe, *J. Chem. Phys.*, **22**, 1430 (1954).

Table IX. Equations of Planes, Distances of Atoms from These Planes, and Dihedral Angles between the Planes[a]

plane no.	A	B	C	D	atom	X	Y	Z	dist, Å	dev, Å
1	−0.4317	−0.1273	−0.8930	−4.1989	Ir[b]	1.3588	1.3051	3.8592	0.000	0.001
					P1[b]	−0.0793	−0.2764	4.7798	0.000	0.005
					P2[b]	−0.3410	2.8728	4.4574	0.000	0.005
					Se1	0.5410	1.3779	1.4563	2.489	0.002
					Se2	2.0234	3.0210	2.1248	1.043	0.002
					P3	3.0856	−0.0777	3.0223	0.178	0.005
					P4	2.7581	1.5701	5.7115	−2.292	0.005
					C1	−1.7073	0.5389	5.0831	0.328	0.018
					C2	−1.5405	1.9967	5.5874	−0.380	0.018
2	0.4251	0.7939	−0.4347	−0.0639	Ir[b]	1.3588	1.3051	3.8592	0.000	0.001
					P3[b]	3.0856	−0.0777	3.0223	0.000	0.005
					P4[b]	2.7581	1.5701	5.7115	0.000	0.005
					Se1	0.5410	1.3779	1.4563	0.755	0.002
					Se2	2.0234	3.0210	2.1248	2.399	0.002
					P1	−0.0793	−0.2764	4.7798	−2.267	0.005
					P2	−0.3410	2.8728	4.4574	0.262	0.005
					C3	4.5243	0.0714	4.1697	0.231	0.019
					C4	4.0117	0.2292	5.6548	−0.507	0.020
3	0.7667	−0.5784	−0.2785	−0.7878	Ir[b]	1.3588	1.3051	3.8592	0.000	0.001
					Se1[b]	0.5410	1.3779	1.4563	0.000	0.002
					Se2[b]	2.0234	3.0210	2.1248	0.000	0.002
					P1	−0.0793	−0.2764	4.7798	−0.444	0.005
					P2	−0.3410	2.8728	4.4574	−2.377	0.005
					P3	3.0856	−0.0777	3.0223	2.357	0.005
					P4	2.7581	1.5701	5.7115	0.404	0.005
4	0.5889	−0.7333	−0.3399	−1.4687	Ir[b]	1.3588	1.3051	3.8592	0.000	
					P1[b]	−0.0793	−0.2764	4.7798	0.000	
					P4[b]	2.7581	1.5701	5.7115	0.000	
					Se1	0.5410	1.3779	1.4563	0.282	
					Se2	2.0234	3.0210	2.1248	−0.277	
					P2	−0.3410	2.8728	4.4574	−2.354	
					P3	3.0856	−0.0777	3.0223	2.316	

plane no.	plane no.	dihedral angle, deg	plane no.	plane no.	dihedral angle, deg
1	2	84.1	2	3	90.7
1	3	90.5	3	4	14.0

[a] The equation of the plane is of the form: $A{*}X + B{*}Y + C{*}Z - D = 0$, where A, B, C, D are constants and X, Y, Z are orthogonalized coordinates. [b] Atoms in plane.

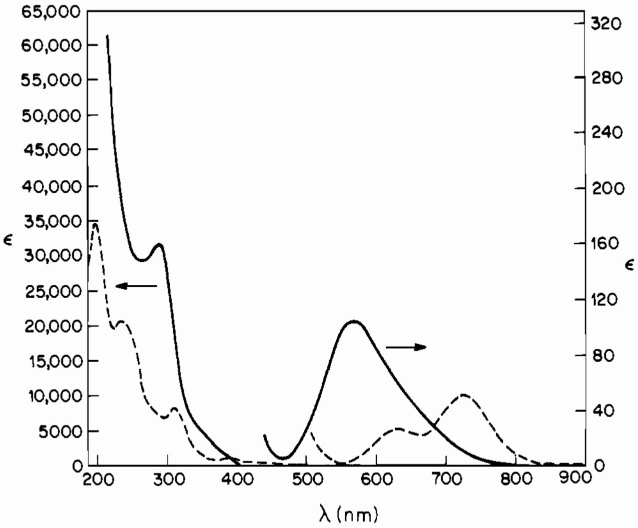

Figure 3. Electronic spectra in acetonitrile solution at 298 K of $[Rh(S_2)(dppe)_2]Cl$ (—) and $[Rh(Se_2)(dmpe)_2]Cl$ (---).

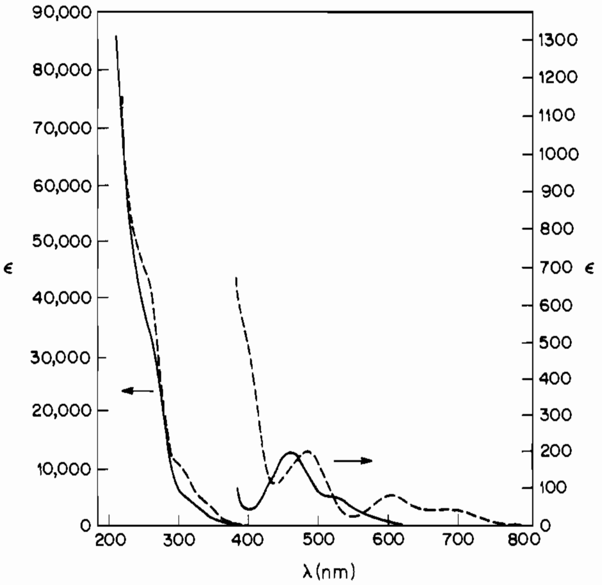

Figure 4. Electronic spectra in acetonitrile solution at 298 K of $[Ir(S_2)(dppe)_2]Cl$ (—) and $[Ir(Se_2)(dppe)_2]Cl$ (---).

phenyl ring transition. In the spectrum of $[Rh(Se_2)(dmpe)_2]Cl$, on the other hand, transitions characteristic of the $[M(X_2)P_4]^+$ core are observed down to 200 nm. Unfortunately, we could not obtain reproducible spectra of $[Rh(S_2)(dmpe)_2]Cl$ and $[Ir(S_2)(dmpe)_2]Cl$.

The lowest energy absorption in the spectra in Figures 3 and 4 is a weak (ϵ 40–100 M^{-1} cm^{-1}) band, which appears at different energies in the different complexes. In some cases the lowest energy feature is a shoulder of another weak band (compounds **1** and **2**) or itself has a weak shoulder (compounds **4** and **7**). A similar weak absorption band (ϵ 100–1000 M^{-1} cm^{-1}) occurs as the lowest energy feature in the spectra of side-on bonded dioxygen complexes, where it has been assigned as $\pi_\perp^* \rightarrow d$ LMCT.[72] Pending completion of detailed mo-

Table X. Comparison of Bond Distances and Angles in $[\mathrm{Ir(Y_2)(dppe)_2}]^+$ Complexes[a]

Y_2	Y-Y′	Ir-Y(Y′)	Y-Ir-Y′	Ir-P(ax)	Ir-P(eq)	P(eq)-Ir-P(eq)′	P(eq)-Ir-Y	P(eq)′-Ir-Y′	ref
O_2	1.52 (1)	2.062 (7) 2.052 (7)	43.4 (3)	2.366 (3) 2.353 (3)	2.308 (3) 2.342 (3)	97.0 (1)	111.8 (2)	108.8 (2)	36
S_2	2.066 (6)	2.422 (4) 2.389 (5)	50.8 (2)	2.371 (5) 2.363 (5)	2.331 (4) 2.337 (4)	98.5 (2)	111.9 (2)	99.8 (2)	6
Se_2	2.312 (3)	2.539 (2) 2.529 (2)	54.3 (1)	2.388 (5) 2.365 (5)	2.327 (5) 2.337 (5)	97.7 (2)	108.0 (1)	101.2 (1)	this work
S_2O_2	2.041[b]	2.413[c] 2.401[c]	50.2	2.388 2.377	2.357 2.365	101.7			31

[a] Bond lengths in angstroms and angles in degrees; numbers in parentheses are estimated standard deviations in the least significant digits. [b] The S-S distance. [c] The Ir-S distance.

Table XI. S-S, Se-Se, M-S, M-Se, M-Halogen, and CO Stretching Frequencies (cm^{-1})[a]

		ν(S-S) or ν(Se-Se)		ν(M-S) or ν(M-Se)		ν(M-halogen)		ν(CO)
no.	compd	IR	Raman	IR	Raman	IR	Raman	IR
1	$[\mathrm{Ir(S_2)(dppe)_2}]\mathrm{Cl}$	(545) (sh)[b]	(542) (ms)[c,d]	308 (vw)[b]	305 (s)[c,d]			
2	$[\mathrm{Ir(Se_2)(dppe)_2}]\mathrm{Cl}$	310 (vw)[b]	308 (m)	182 (vw)[b]	183 (s)			
3	$[\mathrm{Ir(S_2)(dmpe)_2}]\mathrm{Cl}$	510 (wm)	510 (m)		314 (sh), 311 (s)			
4	$[\mathrm{Rh(S_2)(dppe)_2}]\mathrm{Cl}$	(550) (w)[b]	(554) (m)		325 (s)			
5	$[\mathrm{Rh(S_2)(dmpe)_2}]\mathrm{Cl}$	520 (m)	519 (m)		306 (ms, sh)			
6	$[\mathrm{Rh(S_2)(dmpe)_2}]\mathrm{PF_6}$	520 (m)	nm		nm			
7	$[\mathrm{Rh(Se_2)(dmpe)_2}]\mathrm{Cl}$		~300 (sh)	nm	168 (s)			
8	$[\{\mathrm{IrSe_2Cl(CO)(PPh_3)}\}_3]$		*e*		*e*	307 (m, br)[b]	*e*	2041 (s)
9	$[\{\mathrm{IrSe_2Br(CO)(PPh_3)}\}_3]$		*e*		*e*	188 (m, br)[b]	*e*	2038 (s)
10	$[\{\mathrm{IrSe_2Cl(CO)(AsPh_3)}\}_3]$		*e*		*e*	312 (sh)[b]	*e*	2038 (s)
11	$[\{\mathrm{IrS_6Cl(CO)(PPh_3)_2}\}_n]$		487 (s)	316 (sh)[b]	319 (ms)	300 (m)[b]	296 (ms)	2053 (s)
12	$[\{\mathrm{RhS_3Cl(PPh_3)}\}_4]$		*e*	~297 (sh)[b]	*e*	~335 (sh), 307 (br, m)[b]	*e*	
13	$[\{\mathrm{RhS_3Br(PPh_3)}\}_4]$		*e*	300 (sh)[b]	*e*	219 (br, m)[b]	*e*	
14	$[\{\mathrm{RhSe_3Cl(PPh_3)}\}_4]$		*e*		*e*	~340 (sh), 311 (br, m)[b]	*e*	
15	$[\{\mathrm{Rh(S_2)Cl(AsPh_3)}\}_n]$	(507) (sh)	(510) (sh, m)	290 (sh, m)[b]	288 (ms)	334 (s)	346 (s), ~326 (sh)[f]	
16	$[\{\mathrm{Rh(Se_2)Cl(AsPh_3)}\}_n]$		(~285) (sh)		*g*	340 (s), 332 (sh, s)[g]	~340 (sh, s), ~325 (sh)[f]	
17	$[\mathrm{Ir(SI)_2(dppe)_2}]\mathrm{Cl}$	(548) (wm)		~325 (sh), ~300 (vw)	327 (m), ~300 (sh)		ν(S-I) = 218 (vs)	
19	$[\mathrm{(dppe)_2IrS_2Pt(PEtPh_2)_2}]\mathrm{PF_6}$				336 (m), 318 (m)			
25	$[\mathrm{(dppe)_2IrSe_2IrCl(CO)(PEt_2Ph)_2}]\mathrm{Cl}$							2040 (s)
26	$[\{\mathrm{IrSeCl(CO)(PEt_2Ph)_2}\}_2]$							2020 (s)

[a] Values in parentheses are tentative assignments; see discussion in text. Unless otherwise noted, IR frequencies are for samples in CsI disks and Raman frequencies are for rotating polycrystalline samples. Abbreviations: br, broad; m, medium; nm, not measured; s, strong; sh, shoulder; v, very; w, weak. [b] Nujol mull. [c] Nitromethane solution. [d] Strongly polarized band, $\rho = 0.37$. [e] Unable to obtain Raman spectrum; sample decomposed in laser beam. [f] One component of this pair of bands may be due to an X-sensitive vibration of $AsPh_3$. [g] Obscured by strong fluorescence.

Table XII. ^{1}H NMR Data[a]

			$(dppe)_2$ ortho phenyl hydrogen shifts	
no.	compd	τ	intens[b]	J_{P-H}, Hz
1	$[\mathrm{Ir(S_2)(dppe)_2}]\mathrm{Cl}$[c,d]	3.89 (t)	3.6	9
2	$[\mathrm{Ir(Se_2)(dppe)_2}]\mathrm{Cl}$[c,d]	3.82 (t)	3.9	8
4	$[\mathrm{Rh(S_2)(dppe)_2}]\mathrm{Cl}$[e]	3.82 (t)	3.8	8
17	$[\mathrm{Ir(SI)_2(dppe)_2}]\mathrm{Cl}$[f]	3.94 (t)	3.7	9
19	$[\mathrm{(dppe)_2IrS_2Pt(PEtPh_2)_2}]\mathrm{PF_6}$[e]	3.56 (t)	3.9	8

[a] t stands for triplet. Measurements are at the ambient temperature of the NMR probe. [b] Number of protons; determined from intensity = 8(area under triplet/area under CH_2CH_2 absorption) and intensity = 40[area under triplet/(area under triplet + area under main phenyl multiplet)]. [c] Results from reference 70a. [d] In CD_2Cl_2 + ~14% CF_2Cl_2. [e] In CD_3NO_2 solution. [f] In $CDCl_3$ solution.

lecular orbital calculations,[35] we will not attempt to assign the spectra in Table XIII except to note that the calculations support the assignment of the weak low-energy bands as $a_2\pi_\perp^* \rightarrow b_1xz$. However, the b_1xz orbital has more sulfur or selenium than metal character, and the transition is better described as S_2 or Se_2 intraligand, rather than as LMCT as in the dioxygen complexes. $[\mathrm{Ir(O_2)(dppe)_2}]\mathrm{Cl}$ has been reported[73] to have its lowest electronic absorption band at 2.74 μm^{-1} (ϵ 200), strongly blue shifted with respect to the corresponding band of the disulfur and diselenium complexes.

In Table XIII we have assigned numbers to the absorption bands in order to indicate a tentative correlation between the spectra. Bands with the same numbers in the spectra of different compounds are assumed to arise from corresponding transitions. This correlation indicates that the bands are blue shifted on going from a Rh to the corresponding Ir complex but that they are red shifted from an S_2 to the corresponding Se_2 complex.

The lowest energy absorption in the spectrum of $[\mathrm{Ir(SI)_2(dppe)_2}]\mathrm{Cl}$ (Table XIII) is at 2.78 μm^{-1} with ϵ 1.86×10^4 M^{-1} cm^{-1}. There is no evidence of the weak low-energy band

---

(72) A. B. P. Lever and H. B. Gray, *Acc. Chem. Res.*, **11**, 348 (1978).

(73) G. L. Geoffroy, G. S. Hammond, and H. B. Gray, *J. Am. Chem. Soc.*, **97**, 3933 (1975).

Table XIII. Electronic Absorption Spectral Data for $[M(Y_2)(L\text{-}L)_2]Cl$ Complexes[a]

no.	compd	band no.[b]	λ_{max}, nm	$\bar{\nu}_{max}$, μm^{-1}	ϵ, M^{-1} cm^{-1}
1	$[Ir(S_2)(dppe)_2]Cl$	II	525 (sh)	1.90 (sh)	76
		III	458	2.18	194
		V	~320 (sh)	~3.1 (sh)	~4.5 × 10^3
		VII	~260 (sh)	~3.8 (sh)	~3.6 × 10^4
2	$[Ir(Se_2)(dppe)_2]Cl$	I	~675 (sh)	~1.48 (sh)	46
		II	599	1.67	85
		III	480	2.08	198
		IV	~400 (sh)	~2.50 (sh)	~450
		V	~340 (sh)	~2.94 (sh)	~3.8 × 10^3
		VI	~305 (sh)	~3.28 (sh)	~1.0 × 10^4
		VII	~255 (sh)	~3.92 (sh)	~4.4 × 10^4
4	$[Rh(S_2)(dppe)_2]Cl$	II, III	565 (br, asym)[c]	1.77 (br, asym)[c]	106
		V	~360 (sh)	~2.8 (sh)	~4.1 × 10^3
		VI	292	3.45	3.32 × 10^4
		VII	~256 (sh)	~3.90 (sh)	~3.1 × 10^4
7	$[Rh(Se_2)(dmpe)_2]Cl$	II	725	1.38	50
		III	630 (sh)	1.59 (sh)	28
		V	390	2.56	719
		VI	308	3.25	7.93 × 10^3
		VIII	235	4.26	2.18 × 10^4
		IX	199	5.03	3.44 × 10^4
17	$[Ir(SI)_2(dppe)_2]Cl$		360	2.78	1.86 × 10^4
			288	3.47	4.78 × 10^4
			~255 (sh)	~3.92	~5.4 × 10^4
			~240 (sh)	~4.17	~5.7 × 10^4

[a] In CH_3CN solution. [b] The band numbers are intended to indicate a tentative correlation between bands in the different complexes. [c] An unresolved absorption appears to be present on the low-energy side of this band.

Table XIV. Mössbauer Parameters from Least-Squares Analysis of Spectra of $[Ir(Y_2)(dppe)_2]Cl$ and Related Compounds

no.	compd	isomer shift,[a,b] mm/s	quadrupole splitting,[b] mm/s
	$[Ir(O_2)(dppe)_2]Cl$[c]	−0.264 ± 0.01	1.43 ± 0.01
1	$[Ir(S_2)(dppe)_2]Cl$	−0.348 ± 0.005	1.64 ± 0.01
2	$[Ir(Se_2)(dppe)_2]Cl$	−0.407 ± 0.01	1.74 ± 0.01
17	$[Ir(SI)_2(dppe)_2]Cl$	−0.359 ± 0.005	1.56 ± 0.01
19	$[(dppe)_2IrS_2Pt(PEtPh_2)_2]Cl$	−0.422 ± 0.005	1.10 ± 0.01

[a] With respect to iridium metal. [b] Uncertainties are standard errors. [c] A previous report[74a] gives IS = −0.26 ± 0.1 and QS = 1.49 ± 0.1 for the dioxygen complex.

characteristic of the parent disulfur complex.

Absorption spectra of methylene chloride and benzene solutions of compounds **8**, **9**, **15**, and **16** show no evidence of the weak low-energy band expected if terminal side-on bonded S_2 or Se_2 were present.

Mössbauer Spectra. Table XIV summarizes the parameters obtained by least-squares analysis of the Mössbauer spectra, and Figure 5 shows the fits for compounds **1**, **17**, and **19**. All of the compounds studied have similar spectra. In each case there is a single Mössbauer resonance that appears as a doublet because of quadrupole splitting of the $I = {}^3/_2$ ^{193}Ir nuclear ground state. The $I = {}^1/_2$ excited state is unsplit. Since the complexes have ^1A electronic ground states, the splitting is attributed to interaction of the nuclear quadrupole moment with the field gradient due to the ligands, as shielded by the Sternheimer factor.

Since the transition $^{193}Ir({}^1/_2+ \rightarrow {}^3/_2+)$ has a positive value for $\delta\langle r^2\rangle$, the change in mean-square nuclear charge radius,[74] the isomer shift of the 73-keV γ line is directly proportional to $\Delta|\psi(0)|^2$, the difference between the total s-electron densities at the nucleus in the source and absorber. In 5d transition metal complexes changes in $|\psi(0)|^2$ result mainly from changes in the occupancy of 5d and 6s orbitals: 6s electrons directly increase $|\psi(0)|^2$ while 5d electrons decrease it by shielding the s electron from the nucleus. Isomer shift studies have shown that, in phosphine and carbonyl complexes of iridium, charge compensation by the ligands minimizes the change in electronic environment of the metal, which might be expected to accompany a change in the formal oxidation state; in such complexes the formal oxidation state appears to be irrelevant to interpreting the chemistry.[75]

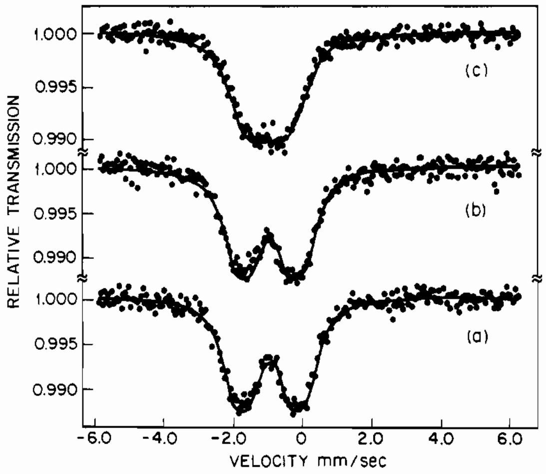

Figure 5. Mössbauer spectra and least-squares fits for (a) $[Ir(S_2)(dppe)_2]Cl$, (b) $[Ir(SI)_2(dppe)_2]Cl$, and (c) $[(dppe)_2IrS_2Pt(PEtPh_2)_2]Cl$.

The decrease in isomer shift for the complexes $[Ir(Y_2)(dppe)_2]Cl$ along the sequence $Y_2 = O_2, S_2, Se_2$ (Table XIV) parallels a decrease in Y_2 electronegativity and indicates that the Ir–Y_2 interaction takes place predominantly via d or p orbitals where shielding effects decrease $|\psi(0)|^2$. A similar rationale applies to the decreased isomer shift of compound **19** compared to that of compound **1**, since oxidative addition across the S–S bond should result in increased S → Ir dona-

---

(74) F. E. Wagner and U. Wagner in "Mössbauer Isomer Shifts", G. K. Shenoy and F. E. Wagner, Eds., North-Holland Publishing Co., Amsterdam, 1978, Chapter 8a.

(75) (a) A. F. Williams, G. C. H. Jones, and A. G. Maddock, *J. Chem. Soc., Dalton Trans.*, 1952 (1975); (b) A. F. Williams, S. Bhaduri, and A. G. Maddock, *ibid.*, 1958 (1975).

tion. The isomer shift of compound **17** is discussed in the following section. Decreasing isomer shift with increasing electron donation to Ir is consistent with the increase in isomer shift with increasing oxidation state found for octahedrally coordinated halogen complexes of iridium.[74] It contrasts with the decrease in isomer shifts with increasing oxidation state found for carbonyl complexes of iridium.[76,77]

Additional Discussion. Side-on bonded disulfur and diselenium in complexes **1–7** can undergo both oxidation and reduction. Examples of oxidation reactions have been given in the Introduction. In these reactions electrons are removed from $S_2\pi^*$ orbitals and the S–S bond is retained in the product, for example, structure VII[31] of $[Ir(SO)_2(dppe)_2]^+$. With one exception, the reactions of compounds **1–7** reported in this paper are all formally reductions of disulfur or diselenium in which the S–S or Se–Se bond is broken. The exception is the reaction of $[Ir(S_2)(dppe)_2]Cl$ with I_2, where we have proposed that the product has structure II, analogous to structure VII. ^1H NMR measurements show the product to have cis-octahedral coordination with equivalent cis groups, and the vibrational spectra show the M–S bonds to be retained. An IR band at 548 cm^{-1} is tentatively assigned as ν(S–S). An important difference between $[Ir(SO)_2(dppe)_2]^+$ and $[Ir(SI)_2(dppe)_2]^+$ is the presence of two additional valence electrons in the latter compound; these presumably occupy the LUMO of the S_2 complex.[35] The presence of electrons in the LUMO, which has significant Ir 5d character, may account for the fact that the isomer shift of the I_2 adduct is slightly more negative than the value for the parent complex, whereas oxidation should have made the shift more positive.

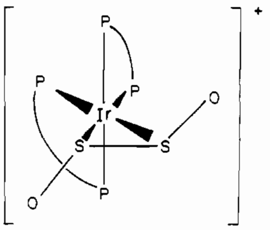

VII

Compounds **8–10**, the trimeric products of the reaction of $IrX(CO)(PPh_3)_2$ (X = Cl, Br) or $IrCl(CO)(AsPh_3)_2$ with Se_8, have a single terminal ν(CO) shifted about 90 cm^{-1} to higher energy compared to that of the starting complex. This indicates that the three iridium atoms are essentially equivalent and that they have undergone oxidative addition. The group added is presumably Se_2 (there is no evidence in the vibrational spectra for coordinated Ph_3PSe or Ph_3AsSe, although a ν(P–Se) or ν(As–Se) frequency could be masked by the strong phenyl bands). However, it is unlikely that the diselenium group is present simply as terminal side-on bonded Se_2, as in structure VIII, since the weak low-energy $\pi_\perp^* \rightarrow xz$ transition expected for this group is not observed in the electronic spectra of compounds **8–10**. A structure that is consistent with all of our observations on compounds **8–10** is shown in IX, where each Se_2 group is coordinated side-on to one Ir atom and also end-on to another Ir atom. The end-on bond utilizes the electrons from the Se_2 $\pi_\perp^*$ orbital, thereby accounting for the absence of a low energy $\pi_\perp^* \rightarrow xz$ transition. The mode of bonding of Se_2 postulated in structure IX has been observed for O_2 in the compound $[\{RhCl(O_2)(PPh_3)_2\}_2]$[78] and for S_2 in the complex $[Mo_4(NO)_4S_{13}]^{4-}$.[22]

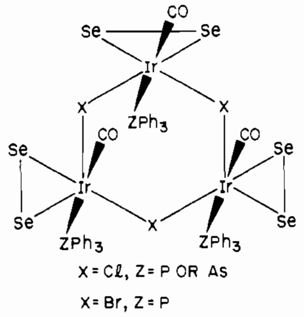

VIII

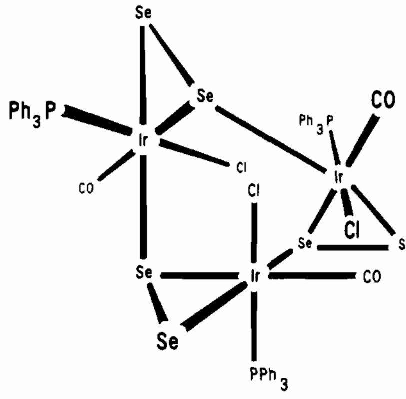

IX

Compounds **12–16** are all obtained in a similar manner from the reaction of S_8 or Se_8 with $RhX(PPh_3)_3$ (X = Cl, Br) or $RhCl(AsPh_3)_3$. The triphenylphosphine complexes have S:Rh or Se:Rh = 3 while the triphenlarsine complexes have S:Rh or Se:Rh = 2. We considered whether this difference was due to the fact that arsines do not react as readily with sulfur and selenium as phosphines, so that compounds **12–14** might contain a Ph_3PS group while compounds **15** and **16** contain only Ph_3As. However, the absence of a ν(P–S) absorption, expected for coordinated Ph_3PS in the range 530–690 cm^{-1}, in the IR spectra of compounds **12** and **13** appears to rule out this explanation.[79] We speculate that compounds **15** and **16** are oligomers of the structural unit X, while compounds **12–14** are oligomers of structural unit XI. Briding disulfur groups of the type suggested in structure X are known in several compounds.[30] The observed conversion of the Ph_3P complex **12** to the Ph_3As complex **15** could occur by chalcogen abstraction by the displaced Ph_3P as shown in the scheme

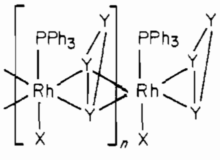

Y = S, Se

X

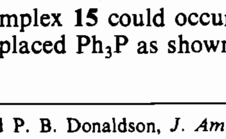

Y = S, Se; X = Cl, Br

XI

---

[76] H. H. Wickman and W. E. Silverthorn, *Inorg. Chem.*, **10**, 2333 (1971).

[77] A. P. Ginsberg, J. W. Koepke, R. L. Cohen, and K. W. West, *Chem. Phys. Lett.*, **38**, 310 (1976).

[78] M. J. Bennett and P. B. Donaldson, *J. Am. Chem. Soc.*, **93**, 3307 (1971).

[79] The IR spectra of compounds **12** and **13** in the 530–690-cm^{-1} region show only a weak phenyl absorption.

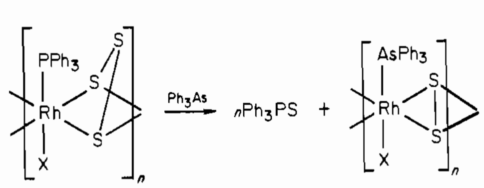

Registry No. **1**, 47898-17-9; **2**, 82522-17-6; **3**, 82522-18-7; **4**, 82522-19-8; **5**, 82522-20-1; **6**, 82522-22-3; **7**, 82522-23-4; **8**, 82522-24-5; **9**, 82544-26-1; **10**, 82522-25-6; **11**, 82536-82-1; **12**, 82522-27-8; **13**, 82522-29-0; **14**, 82522-31-4; **15**, 82522-33-6; **16**, 82522-35-8; **17**, 82522-36-9; **18**, 82522-37-0; **19**, 82536-84-3; **20**, 82522-38-1; **21**, 31168-83-9; **22**, 82522-39-2; **23**, 74472-62-1; **24**, 82522-40-5; **25**, 82522-41-6; **26**, 82522-42-7; $[Ir(Se_2)(dppe)_2]Cl\cdot H_2O\cdot 0.5C_6H_6$, 82522-43-8; S_8, 10544-50-0; $[Ir(dppe)_2]Cl$, 15390-38-2; Se_8, 12597-33-0; $[Ir(dmpe)_2]Cl$, 60314-45-6; $[Rh(dppe)_2]Cl$, 15043-47-7; $[Rh(dmpe)_2]Cl$, 16884-41-6; $[IrCl(CO)(PPh_3)_2]$, 14871-41-1; $[IrBr(CO)(PPh_3)_2]$, 14970-06-0; $[IrCl(CO)(AsPh_3)_2]$, 15682-62-9; $RhCl(PPh_3)_3$, 14694-95-2; $RhBr(PPh_3)_3$, 14973-89-8; $[RhCl(AsPh_3)_3]$, 14973-92-3; $Pt(PPh_3)_3$, 13517-35-6; $Pt(PEtPh_2)_3$, 36464-08-1; $[Ir(Se)_2(dppe)_2]BPh_4$, 82522-45-0; $[Pt(PEtPh_2)_4]$, 70163-52-9; $[IrCl(CO)(PEt_2Ph)_2]$, 27488-97-7; $[\{RhSCl(PPh_3)\}_n]$, 82536-86-5; $PEtPh_2$, 607-01-2; PPh_3, 603-35-0; Hg, 7439-97-6.

Supplementary Material Available: Tables of observed and calculated structure factors and thermal parameters (14 pages). Ordering information is given on any current masthead page.

Contribution from the Department of Chemistry,
University of Queensland, Brisbane, Australia 4067

Tetraglycine Complexes of Cobalt(III): Preparations, ^1H and ^{13}C NMR Spectra, Absorption Spectra, and Reactions in Acid

CLIFFORD J. HAWKINS* and M. TERRY KELSO

Received May 11, 1981

The preparations of three cobalt(III) complexes of tetraglycine are reported. In one complex, $[Co(NH_3)_2(H_{-3}GGGG)]^-$, the peptide is coordinated as a quadridentate through the terminal NH_2 and three peptide nitrogens. In the other two complexes, $[Co(NH_3)_3(H_{-2}GGGG)]$ and $[Co(NH_3)_3(H_{-1}GGGGH)]^{2+}$, the peptide is a terdentate chelate coordinated in the former through the terminal NH_2 and two peptide nitrogens and in the latter through the terminal NH_2, the adjacent peptide nitrogen, and a peptide oxygen. The ^1H and ^{13}C NMR spectra are given for the free peptide in its anionic, zwitterionic, and cationic forms and for the cobalt(III) complexes. The chemical shift data are analyzed in terms of the effects of protonation and coordination. In acid the free carboxylate in $[Co(NH_3)_2(H_{-3}GGGG)]^-$ is protonated with a pK_a at 278 K of 4.40 ± 0.08. At higher acid concentrations the terminal peptide nitrogen of the quadridentate chelate is protonated (pK_a at 298 K and $I = 0.25$, 1.7) and the nitrogen dissociates with a rate constant of 7.2×10^{-3} s^{-1} at 298 K ($I = 0.25$). The resultant diammineaqua complex with the chelate bound through the terminal NH_2 and two peptide nitrogens and the analogous triammine complex undergo a coordination rearrangement reaction in acid that involves an initial protonation (pK_a at 298 K and $I = 0.25$, 1.0) followed by the interchange of the Co–N to Co–O bonding for the peptide group trans to the NH_2 group with rate constants of 1.6×10^{-5} and 2.5×10^{-5} s^{-1}, respectively.

Introduction

The only cobalt(III) tetrapeptide complex in the literature, $[Co(dien)((H_{-1}GGGG)OEt)]^{2+}$, has the peptide coordinated as a terdentate chelate coordinated via the NH_2 group, a deprotonated peptide nitrogen, and a peptide oxygen.[1,2] The first quadridentate peptide complex of cobalt(III) was reported recently for a series of tripeptides.[3] In the present paper, the preparations are given for $[Co(NH_3)_2(H_{-3}GGGG)]^-$, in which the tetrapeptide is coordinated as a quadridentate through the NH_2 and three peptide nitrogens, and for triammine complexes where the peptide is a terdentate through the NH_2 and two peptide nitrogens, and through the NH_2, one peptide nitrogen, and one peptide oxygen. The UV–visible absorption and ^1H and ^{13}C NMR spectra of these complexes are also presented, and the NMR spectra are compared to those of the free peptide to determine the effects of coordination.

Margerum and his co-workers have studied the reactions with acid of a series of labile peptide complexes.[4–6] The peptide donor groups were found to be progressively removed from the metal. Because of the lability of the complexes, the various intermediates have not been isolated. However, the inertness of the present cobalt(III) system allows the isolation of complexes with the intermediate structures. The kinetics of the reactions with acid of the cobalt(III) tetraglycine complexes are also reported in this study.

Experimental Section

Materials. Tetraglycine was purchased from ICN Pharmaceuticals, Inc., and was used without further purification. All other reagents were of AnalaR grade. Stock solutions of perchloric acid were standardized by titration with standard CO_2-free sodium hydroxide solutions using an E.I.L. Vibron 39A pH meter. For the kinetics a constant ionic strength of 0.25 was maintained by the addition of appropriate amounts of dry sodium perchlorate. Adsorption properties of the complexes on ion-exchange cellulose papers were used to determine the sign of the charge on the complexes. Carboxymethyl cation-exchange cellulose CM 82 and aminoethyl anion-exchange cellulose AE 81 were used for this work. The pK_a value for the terminal carboxylate group was determined at 298 K by titration with standard acid using the above pH meter.

---

(1) The ligand abbreviations are as follows: dien, diethylenetriamine; GGGG, tetraglycinate; GGG, triglycinate; GG, diglycinate. For a peptide X, HX represents the peptide in the zwitterionic form, XH represents the peptide with the carboxylate protonated, and $H_{-n}X$ represents the peptide with n peptide nitrogens deprotonated. With use of this nomenclature, and with the premises that the amine group is preferentially coordinated, the deprotonated nitrogens are coordinated, and a coordinated peptide oxygen can only be a terminal group in the coordination, a formula $[CoA_3(H_{-1}GGGG)]^{n+}$ would depict a complex in which the amine, a peptide nitrogen, and a peptide oxygen are coordinated in that order.

(2) Wu, Y.; Busch, D. H. *J. Am. Chem. Soc.* **1972**, *94*, 4115.

(3) Evans, E. J.; Grice, J. E.; Hawkins, C. J.; Heard, M. R. *Inorg. Chem.* **1980**, *19*, 3496.

(4) Paniago, E. G.; Margerum, D. W. *J. Am. Chem. Soc.* **1972**, *94*, 6704.

(5) Pagenkopf, G. K.; Margerum, D. W. *J. Am. Chem. Soc.* **1968**, *90*, 6963.

(6) Cooper, J. C.; Wong, L. F.; Margerum, D. W. *Inorg. Chem.* **1978**, *17*, 261.

0020-1669/82/1321-3681$01.25/0